Multi-User Relay Selection for Full-Duplex Radio

Saman Atapattu, *Member, IEEE*, Prathapasinghe Dharmawansa, *Member, IEEE*, Marco Di Renzo, *Senior Member, IEEE*, Chintha Tellambura, *Fellow, IEEE*, and Jamie S. Evans, *Senior Member, IEEE*

***Abstract*— This paper investigates a user-fairness relay selection (RS) problem for decode-and-forward (DF) full-duplex (FD) relay networks, where multiple users cooperate with multiple relays in each coherence time. We consider two residual self-interference (RSI) models with or without direct links. We propose a sub-optimal relay selection (SRS) scheme which requires only the instantaneous channel state information (CSI) of source-to-relay and relay-to-destination links. To evaluate the performance, the outage probability of SRS is derived for different scenarios depending on RSI models and the availability of direct links. To further investigate, asymptotic expressions are derived for the high-transmit power regime. For comparison purposes, 1) the average throughputs of the FD and half-duplex (HD) modes are derived; 2) non-orthogonal transmission is considered and its performance is discussed with approximations; and 3) the impact of imperfect CSI is investigated with the aid of analysis. While simulation results are provided to verify the analytical results, they reveal interesting fundamental trends. It turns out that a significant throughput degradation occurs with FD mode over HD mode when self-interference is fully proportional to the transmit power. Since all users can communicate in the same coherence time with the FD mode, these joint RS schemes are useful for user-fairness low-latency applications.**

***Index Terms*— Full-duplex communications, multiple-user networks, outage probability, relay selection, residual self-interference, throughput.**

I. Introduction

CONVENTIONAL wisdom had been that a radio node cannot simultaneously transmit and receive on the same frequency band. Recently it has been discovered that full-duplex (FD) radio not only able do that, but also avoids typical spectrum splitting employed across forward and reverse links and hence improves spectrum efficiency compared to conventional half-duplex (HD) radio in which silent times lead to a loss of spectral efficiency (also known as the multiplexing loss) [1]. For instance, FD nodes relaying can potentially double the spectral efficiency achieved by the conventional HD relaying, thereby extending network coverage while improving power efficiency and robust connectivity [2]. However, since the self-interference (SI) signal on a FD node can sometimes be 100 dB above its legitimate received signal strength, the benefits of FD radio are contingent on proper SI cancellation [3]. Nevertheless, the measurement and fully suppression of SI is challenging even with the recent signal processing breakthroughs [4].

Although multiple relays can improve error-rate and link-reliability by exploiting multipath diversity, overall spectral efficiency can be affected because of the need for one orthogonal channel per each relay. This in turn increases bandwidth utilization, time slots or spreading codes. On the other hand, because relay selection (RS) schemes activate only one or few relays from a large set of nodes, resource utilization and overhead do not scale up as rapidly. Instead, RS enjoys the best of both techniques, e.g., spectral efficiency and full diversity gains [5]–[7]. Although RS requires an exchange of channel state information (CSI) between the nodes, such multiplexing losses can be recovered under the constraint of very limited feedback [8]. The RS with FD radios is important because it provides better diversity-multiplexing gain tradeoff (DMT) at least at the high multiplexing gain regime where the FD achieves a better multiplexing gain than that of the HD [9]. Effective FD RS strategies are thus the main focus of this paper.

A. Related Work

FD RS strategies have been considered for one-way communication [10]–[14], two-way communication [15]–[17], cognitive radio [18], device-to-device (D2D) [19], physical-layer security [20], energy harvesting [21], [22], and non-orthogonal multiple access (NOMA) [23], to mention but a few. Outage probability and asymptotic analysis of several RS schemes which are based on the available channel state information (CSI) are derived in [10]. A joint RS and power allocation with outdated CSI is analyzed in [11]. Outage probability, average symbol error rate, and ergodic capacity are derived for a joint relay and transmit/receive antenna mode selection scheme

Manuscript received April 6, 2018; revised July 29, 2018 and September 25, 2018; accepted October 9, 2018. Date of publication October 22, 2018; date of current version February 14, 2019. This work is supported in part by the Australian Research Council (ARC) through the Discovery Early Career Researcher (DECRA) Award under Grant DE160100020 and in part by the Discovery Project (DP) under Grant DP180101205. The associate editor coordinating the review of this paper and approving it for publication was X. Chen. *(Corresponding author: Saman Atapattu.)*

S. Atapattu and J. S. Evans are with the Department of Electrical and Electronic Engineering, The University of Melbourne, Melbourne, VIC 3010, Australia (e-mail: saman.atapattu@unimelb.edu.au; jse@unimelb.edu.au).

P. Dharmawansa is with the Department of Electronic and Telecommunication Engineering, University of Moratuwa, Moratuwa 10400, Sri Lanka (e-mail: prathapa@uom.lk).

M. Di Renzo is with the Laboratoire des Signaux et Systmes, CentraleSuplec, Universit Paris-Saclay, 91192 GifsurYvette, France (e-mail: marco.direnzo@lss.supelec.fr).

C. Tellambura is with the Department of Electrical and Computer Engineering, University of Alberta, Edmonton, AB T6G 2V4, Canada (e-mail: chintha@ece.ualberta.ca).

Color versions of one or more of the figures in this paper are available online at http://ieeexplore.ieee.org.

Digital Object Identifier 10.1109/TCOMM.2018.2877393

in [12]. In [13], channel capacities with RS are analyzed under different adaptation policies including optimum power with rate-adaptation and truncated channel inversion with a fixed rate. For nodes distributed as a 2-D homogeneous Poisson point process, an analytical framework is proposed to study how RS strategies perform with HD and FD nodes by combining renewal theory and stochastic geometry in [14]. In [15], an optimal RS scheme which maximizes the effective signal-to-interference and noise ratio (SINR) is proposed and analyzed for a two-way FD relay network. In [17], outage probability based on max-min scheduling is analyzed for a two-way multiple-user network where user pairs compete only for one relay node. A multi-source multi-relay network is considered with one destination for two-way network in [16], where the best source is selected based on the instantaneous signal-to-noise ratio (SNR) of the direct link and the best relay is selected by using the max-min principle based on the selected source. However, there is no simultaneous transmission from all source nodes.

Optimal RS for the FD underlay cognitive radio networks is analyzed with respect to the distributional properties of the received SNR in [18]. A power-efficient RS scheme is formulated as a combinatorial optimization problem to minimize the power consumption of the mobile devices in multiple D2D user pairs in [19]. The secrecy outage probability of a hybrid RS scheme which switches between FD and HD modes is studied in [20]. The FD RS for physical-layer security in a multi-user network is recently considered under the attack of colluding eavesdroppers in [24]. RS schemes for FD relay networks with energy harvesting are considered for the power-splitting protocol in [21] and the time-switching protocol in [22]. In [23], the impact of RS on cooperative NOMA is also investigated for both FD and HD modes by considering the locations of relays where stochastic geometry tools are used.

B. Problem Statement

As discussed above, in the existing literature, FD RS problems are limited to two scenarios: i) single source-destination pair with multiple intermediate relays; ii) multiple sources and multiple relays with single destination where only one selected source communicates with the destination; or iii) multiple source-destination pairs with single intermediate relay where only one pair communicates at each coherent time [25]. However, the model of single source-destination pair per coherence time has limited applications as wireless systems evolve from Long Term Evolution (LTE) to fifth generation (5G), the number of active users per unit area is expected to increase dramatically, making simultaneous communication is a more urgent goal, with better resource utilization, supporting ultra-reliable low-latency communication (URLLC) [26].

In FD relay studies [10], [11], it is commonly assumed that no direct source-destination link exists because the direct link is sufficiently weak due to obstacles and/or deep fading. In HD relaying, however, a direct link is a great advantage as the destination receives two copies of the same signal. However, in FD mode, the relayed received signal at the destination is the previous signal of the source. Unless the source employs a smart strategy, e.g., coding such as space-time code (STC), or destination employs a smart receiving technique, e.g., buffering, this relayed signal interferes with the direct-link received signal at the same time instance [27]–[30]. In [31], the outage probability is derived for a basic three-node FD relay network with direct link over Rayleigh fading channels under distance-dependent path loss. Those results reveal that the FD relay network can achieve the full diversity order only when the self-interference is independent of transmit power and when there is no direct link. In all other cases, diversity gains are lost and an outage floor occurs. Since existing FD RS is limited to single source-destination pair, FD RS must be developed for multiple source-destination pairs communicating via intermediate relays. Availability of direct links and their interference are a special case of this problem. This typical scenario has general applications in future wireless systems, and the related FD RS has remained widely open to date. Therefore, given this state-of-the-art, we address this problem.

C. Challenges and Contributions

With FD RS for multiple user pairs, we find the following two challenges:

i) When a given relay cannot be shared by more than one user and limited channel state information (CSI) is available, the first challenge is to develop an RS scheme which improves each individual user link as well as user fairness. User fairness refers to the potential equality of quality of service (QoS) parameters among different users. In our problem, maximizing the SINR of the worst-case link is a possible way to ensure fairness among the users. For example, randomly choosing a relay, the simplest RS scheme, does not need CSI but offers no performance gains. On the other hand, with full CSI availability, a naive RS strategy is to rank the best relays and assign them to the users one by one. This scheme clearly ensures QoS imbalances among users. Focusing on user fairness, [32]–[34], respectively, proposed and developed RS algorithms to find the set of paths that maximizes the minimum end-to-end SINR of all users for a full-CSI HD network and for a full-CSI FD network. A crucial step in in-band FD communications is the full-CSI estimation of time-varying self-interference channels at relays and direct channels at destinations. Thus, in practice, full-CSI may not be available at a central node (relay selector) to perform such RS.

ii) The second challenge is the myriad of analytical difficulties inherent in performance evaluation as all possible user SINRs via multiple relays (see (4)) are non-identical and also correlated random variables (rvs). In particular: i) For a given user pair, a common direct link exists with multiple relay links. Consequently, all possible end-to-end SINRs via all relays are correlated due to this common direct link, i.e., entries of each row of (4); and ii) For a given relay, a common self-interference channel exists for all users, and all possible end-to-end SINRs from all user

pairs via a given relay are correlated due to this common SI, i.e., entries of each column of (4). Since the analysis involves the order statistics of correlated rvs, this multi-user RS problem is radically different from traditional RS problems. This correlation among the rvs may also be another reason for the lack of analysis of multi-user FD networks thus far in the literature.

To address these challenges, this paper studies the RS problem for multiple source-destination pairs and multiple DF relays. In this respect, a recent paper [34] considered Gaussian SI channels and having no direct links among source-destination pairs. In contrast, in this paper, we consider the more general scenario that the SI channel may either be Gaussian noise or a random (fading) channel, and that direct links may exist between source-destination pairs. The key technical contributions are:

1) From practical point of view, we may reasonably assume that the relay selector does not have knowledge of instantaneous direct channels and SI channels, but has partial knowledge of them (statistics). Based on this realistic assumption, we propose a sub-optimal relay selection (SRS) scheme, which becomes equivalent to optimal relay selection (ORS) if there are no source-destination direct links and the SI channels are Gaussian.
2) We derive closed-form outage probability of FD SRS considering Rayleigh fading channels and for four different scenarios based on SI models and the availability of direct links. Asymptotic analysis is also provided to ascertain the diversity order and the outage floor.
3) The average throughput of FD SRS is also derived for comparison purposes. In particular, we compare it with the HD mode, and also with interfering non-orthogonal transmissions from source and relay nodes.

The rest of this paper is organized as follows. Section II discusses the system model and RS scheme. Section III derives the SRS performance analysis with exact and asymptotic outage probabilities, and the average throughput. Section V presents numerical results and discussions, followed by the conclusions in Section VI. The respective proofs are relegated to the Appendix.

II. System Model

A. Network Model and assumptions

This work considers a general multiple source-destination pairs dual-hop wireless relay network (Fig. 1), where the K sources $S_1, \ldots, S_K$ (source-cluster) communicate with their corresponding destinations $D_1, \ldots, D_K$ (destination-cluster) via FD relays $R_1, \ldots, R_N$ (relay-cluster). Thus, we have K user pairs, denoted as user k, $k \in \{1, \ldots, K\}$. Each source node and each destination node are single-antenna nodes. Each FD relay has one transmit antenna and one receive antenna. The power budget is fixed at p for each source and relay. Different power levels can be considered for power allocation problems, e.g. [35]. We assume that each user is helped by one and only one relay, and each relay can help at most one user. Thus, we need $N \geq K$.[1] To avoid interference among users, the users are assigned orthogonal channels using frequency-division or time-division multiple access. It is also important to note that almost all FD RS papers in the literature omit the direct link by assuming that the direct channel is sufficiently weak to be ignored due to obstacles and/or deep fading, e.g., [10]–[14]. Unless we use an advanced signal processing technique at the destination, the direct link signal is interference to the FD relay signal. While this is a widely accepted assumption in the literature, in practice, we may still have an impact from weaker direct links in wireless environments due to multipath propagation. We thus consider a more general multiple-user and multiple-FD-relay network with and without direct links as shown in Fig. 1. To treat the direct link signal as a useful signal in FD RS, we need different signal processing techniques and joint resource allocations which moves this situation beyond the scope of this paper.

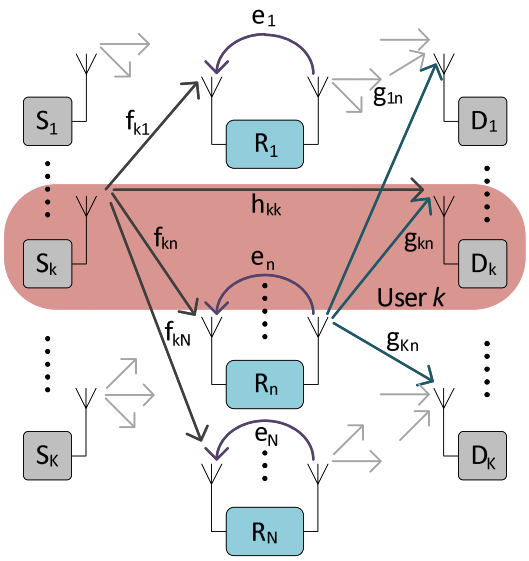

Fig. 1. A full-duplex multiple-user pairs network with multiple relays.

We assume independent small-scale multipath Rayleigh fading for all the links along with large-scale path-loss fading. Further, the distance between clusters is much larger than the distance between the nodes in the same cluster. Therefore, the channel gains and distances in a given hop are identical while the channel gains and distances of the two hops are not necessarily identical. The fading coefficient, channel variance and distance between S_k and R_n (the first hop) are f_{kn}, σ_f^2 and l_{sr}, respectively. Thus, all the f_{kn}'s are independent and identically distributed (i.i.d.) zero-mean complex Gaussian

[1]The scenario $K > N$ should be treated separately due to a number of reasons. If each relay can help at most one user, in each coherence time, only N users can be selected, e.g., random-user selection or best-N-users selection. If each relay can help more than one user, all K users can communicate in every coherence time by jointly allocating relays and powers. If there are direct links, any user can communicate with its destination via either the direct link or a relay link where at least $(K - N)$ users can use their direct links, given that the direct-link carries useful information. Given these complexities, the scenario $K > N$ is beyond the scope of this paper and left as future research.

with $\mathcal{CN}(0,\sigma_f^2)$ for $n \in \{1,\ldots,N\}$ and $k \in \{1,\ldots,K\}$. Similarly, these parameters between R_n and D_k (the second hop) are g_{kn}, σ_g^2 and l_{rd}, respectively, i.e., $g_{kn} \sim \mathcal{CN}(0,\sigma_g^2)$. Further, those parameters of the direct link of user k are h_k, σ_h^2 and $l_{sd}(\leq l_{sr}+l_{rd})$, respectively, i.e., $h_k \sim \mathcal{CN}(0,\sigma_h^2)$. Since reception and transmission occur simultaneously, the R_n relay receives a self-interference via its channel e_n. Moreover, f_{kn}, g_{kn}, h_k, and e_n are independent but not necessary identical.

B. Analytical Model

Without loss of generality, the user k helped by R_n is elaborated here. We denote the information symbols of the source S_k and the relay R_n as x_{s_k} and x_{r_n}, respectively, with unit average energy ($\mathbb{E}\left[|x_{s_k}|^2\right]=1$ where $\mathbb{E}[\cdot]$ is the expectation). At time t, the received signal at R_n is $y_{r,n}[t] = \sqrt{\frac{p}{l_{sr}^{\eta}}} f_{kn} x_{s_k}[t] + i_n[t] + n_{r,n}[t]$, $n=1,\ldots,N$, where η is the path loss exponent, $n_{r,n}[t]$ is the additive white Gaussian noise (AWGN) at R_n with zero-mean and σ_r^2 variance, and $i_n[t]$ is the self-interference term.

Residual self-interference (RSI) models: If no interference cancellation is performed at R_n, we may write $i_n[t] = \sqrt{p} e_n x_{r_n}[t]$ and $x_{r_n}[t] = \hat{x}_{s_k}[t-1]$. Here, the symbol $\hat{x}_{s_k}[t-1]$ represents the decoded and forwarded information symbol at the relay R_n which was transmitted by S_k in the previous time-slot at time $(t-1)$. Then the signal $i_n[t]$ can dominate $y_{r,n}[t]$ and can cause significant performance degradation [36]. To avoid this, each relay node applies some self-interference cancellation, which results in RSI denoted as $\tilde{i}_n[t]$.

To avoid excessive interference, each relay node applies some self-interference cancellation, which results in RSI denoted as $\tilde{i}_n[t]$ [37], [38]. The antenna isolation techniques such as implementing a solid physical barrier between transmit and receive antennas, utilizing directional antennas and exploiting antenna polarization greatly mitigate the transmit power leakage especially via the line-of-sight (LoS) path. However, there still exists RSI which is received due to the non-LoS multi-path propagation. Among different options, the following two RSI models which are often used in the literature are adopted in this paper:

1) RSI Model I: $\tilde{i}_n[t]$ is a block-fading complex Gaussian $\mathcal{CN}(0,\sigma_i^2)$ variable, and the amplitude of RSI is thus Rayleigh distributed. This model is valid when the transmit signal from a relay returns to its receive antenna via different multi-paths, and is used in [10]–[12] and many more papers.
2) RSI Model II: $\tilde{i}_n[t]$ is i.i.d. with zero-mean, σ_i^2 variance, additive and Gaussian, which has similar effect as AWGN [2]. Based on the central limit theorem, the Gaussian assumption holds in practice due to the various sources of imperfections in the interference cancellation process. This model is extensively used in the literature, e.g., [2], [13], [16].

For performance analysis over block fading channels, the RSI term is treated as a random variable only under Model I. Further, the variance of the RSI depends on relay transmit power and the SI cancellation technique. Since all relays have the same transmit power P and the similar SI cancellation technique is implemented at each FD radio, it is reasonable to assume that RSI samples of all relays are i.i.d. By including the impacts of several stages of cancellation into the RSI variance, in general, it is modeled as $\sigma_i^2 = \omega p^{\nu}$ where the two constants, $\omega > 0$ and $\nu \in [0,1]$, depend on the SI cancellation scheme used at the relay [2]. One can thus investigate the effect of RSI based on three cases: i) $\nu = 0$; ii) $\nu = 1$; and iii) $0 < \nu < 1$. In terms of performance, the cases $\nu = 0$ and $\nu = 1$ represent the best-case scenario and the worst-case scenario, respectively. Since the performance of the case $0 < \nu < 1$ is in-between those two cases [34], in this paper, we only consider $\nu = 0$ and $\nu = 1$.

We also define $\alpha_{kn} = |f_{kn}|^2$; $\beta_{kn} = |g_{kn}|^2$; $\delta_k = |h_k|^2$; and $\epsilon_n = |\tilde{i}_n|^2$. Then, we write channel gains in the first-hop, second-hop, direct and self-interference links, respectively, as $\mathbf{H_1} = (\alpha_{kn}) \in \mathbb{R}^{K\times N}$; $\mathbf{H_2} = (\beta_{kn}) \in \mathbb{R}^{K\times N}$; $\mathbf{D} = (\delta_k) \in \mathbb{R}^{K\times 1}$; and $\mathbf{I} = (\epsilon_n) \in \mathbb{R}^{N\times 1}$. With the DF relay R_n, the received signal at D_k is $y_{d,k}[t] = \sqrt{\frac{p}{l_{rd}^{\eta}}} g_{kn} x_{r_n}[t] + \sqrt{\frac{p}{l_{sd}^{\eta}}} h_k x_{s_k}[t] + n_{d,k}[t]$, $\forall k$, where $n_{d,k}[t]$ is the AWGN at D_k with zero-mean and σ_d^2 variance. Since D_k interests on the relay signal $x_{r_n}[t]$, the direct link signal $x_{s_k}[t]$ is an interference. Thus, the receive SINRs at relay R_n (the first hop) and the destination D_k (the second hop) can be given, respectively, as

$$\gamma_{kn,1} = \begin{cases} \dfrac{a\alpha_{kn}}{1+c\epsilon_n} = \dfrac{x_{kn}}{1+u_n}; & \text{Model-I;} \\ \dfrac{a\alpha_{kn}}{1+c\sigma_i^2} = \dfrac{x_{kn}}{1+c\sigma_i^2}; & \text{Model-II,} \end{cases}$$
$$\gamma_{kn,2} = \begin{cases} \dfrac{b\beta_{kn}}{1+d\delta_k} = \dfrac{y_{kn}}{1+v_k}; & \text{with direct link;} \\ b\beta_{kn} = y_{kn}; & \text{without direct link,} \end{cases} \quad (1)$$

respectively, where $a = \frac{p}{l_{sr}^{\eta}\sigma_r^2}$; $b = \frac{p}{l_{rd}^{\eta}\sigma_d^2}$; $c = \frac{1}{\sigma_r^2}$; $d = \frac{p}{l_{sd}^{\eta}\sigma_d^2}$; $x_{kn} = a\alpha_{kn}$; $y_{kn} = b\beta_{kn}$; $u_n = c\epsilon_n$; and $v_k = d\delta_k$. Thus, random variable $Z \in \{x_{kn}, y_{kn}, u_k, v_n\}$, is Exponential probability density function (p.d.f.) and cumulative distribution function (c.d.f.) given by

$$f_Z(z) = \lambda e^{-\lambda z} \quad \text{and } F_Z(z) = 1 - e^{-\lambda z}. \quad (2)$$

Here, the parameter λ for $Z \in \{x_{kn}, y_{kn}, u_n, v_k\}$ denoted by $\lambda \in \{\lambda_x, \lambda_y, \lambda_u, \lambda_v\}$, respectively, takes the value $\lambda_x = \frac{1}{a\sigma_f^2}$; $\lambda_y = \frac{1}{b\sigma_g^2}$; $\lambda_u = \frac{1}{c\sigma_i^2}$; and $\lambda_v = \frac{1}{d\sigma_h^2}$.

The effective end-to-end receive SINR of user k helped by the DF relay R_n is given by[2]

$$\gamma_{kn} = \min\left(\gamma_{kn,1},\, \gamma_{kn,2}\right). \quad (3)$$

Thus, all possible user SINRs connected via any relay can be given in matrix form as

$$\mathbf{\Gamma} = (\gamma_{kn}) \in \mathbb{R}^{K\times N}. \quad (4)$$

[2]For AF relaying, the effective end-to-end receive SINR of user k can be given by $\gamma_{kn}^{\text{AF}} = \frac{\gamma_{kn,1}\,\gamma_{kn,2}}{\gamma_{kn,1}+\gamma_{kn,2}+1}$. Since this can be upper-bounded as $\gamma_{kn}^{\text{AF}} \leq \min\left(\gamma_{kn,1},\, \gamma_{kn,2}\right)$, the results in this paper can be used as approximations for AF relaying, especially in moderate and high SINR regions.

C. Max-Min Fairness Relay Selection (RS) Scheme

From Fig. 1, it is seen that each user has N possible paths (relays). Since a relay cannot be shared between more than one user, for a given relay assigned to one user, there are $(N-1)$ possible relays for any next user. Likewise, there are $(N-K+1)$ possible paths for the final user. We can thus consider several possible RS schemes. But we know that random RS has no performance improvement and naive RS causes significant performance degradation for the final user compared to the other users. Thus, we need an RS scheme, which guarantees the individual performance as well as user fairness, capable of choosing the set of paths that maximizes the minimum end-to-end SINR of all users. Such an algorithm is proposed for an HD relay network in [39]. Further developed algorithm in [32] maximizes the minimum receive SINR of all users, and guarantees an unique solution. The algorithm can be performed on entries of the matrix $\mathbf{\Gamma}$.

- Optimal RS (ORS) with global CSI: If a central node (which may also be one of the nodes in given network) has global channel knowledge, i.e., $f_{kn},\ g_{kn},\ h_k$ and $\tilde{i}_n\ \forall k,n$, to calculate $\mathbf{\Gamma}$, the RS matrix for the ORS scheme $\mathbf{\Gamma}_o$, i.e., max-min optimal, can be defined as

$$\mathbf{\Gamma}_o = \mathbf{\Gamma} = (\gamma_{o,kn}) \in \mathbb{R}^{K\times N} \text{ where } \gamma_{o,kn} = \gamma_{kn}. \quad (5)$$

- Sub-optimal RS (SRS) with some local CSI: A crucial step in in-band FD communications is the estimation of time-varying self-interference channels, for which we need periodic estimation and reporting. Similarly the destination may not have any knowledge of the source transmission. Thus, from the practical point of view, we may reasonably assume that the relay selector: i) has instantaneous knowledge of f_{kn} and $g_{kn}\ \forall k,n$; and ii) does not have instantaneous knowledge of h_k and $\tilde{i}_n\ \forall k,n$, but has their partial knowledge, i.e., with known statistic σ_h^2 and σ_i^2. Based on these assumptions and known distances, the RS matrix for the SRS scheme $\mathbf{\Gamma}_s$ is defined as

$$\mathbf{\Gamma}_s \triangleq (\gamma_{s,kn}) \in \mathbb{R}^{K\times N} \quad (6)$$

where

$$\gamma_{s,kn} = \min\left(\kappa\,\alpha_{kn}, \mu\,\beta_{kn}\right);\quad \kappa = \frac{a}{1+c\sigma_i^2};$$

$$\mu = \begin{cases} \dfrac{b}{1+d\sigma_h^2}; & \text{with direct link;} \\ b; & \text{no direct link.} \end{cases}$$

Upon calculating the RS matrices $\mathbf{\Gamma}_o$ and $\mathbf{\Gamma}_s$, the RS can be developed by extending the proposed algorithm in [39] and further extended algorithm in [32] as following two steps:

- Step I: For $\mathbf{\Gamma}_o$ for $\mathbf{\Gamma}_s$, we apply `Main algorithm` in [39, Fig. 5] to maximize the minimum SINR across the users. Denoted by u (and R_u), the user (and associated relay) achieving the optimum.
- Step II: Since Step I may not maximize other users' SINRs, in this step, the u-th row and corresponding R_u's column are deleted from $\mathbf{\Gamma}_o$ or $\mathbf{\Gamma}_s$, denoted as $\mathbf{\Gamma}_{o,u}$ or $\mathbf{\Gamma}_{s,u}$, respectively, and then `Main algorithm` in [39, Fig. 5] is performed on $\mathbf{\Gamma}_{o,u}$ or $\mathbf{\Gamma}_{s,u}$. This is iterated until all users are associated to a relay.

These two steps guarantee the uniqueness of the solution. This algorithm first optimizes the worst user's SINR, then the second worst user and so on, see [32], [39] for details. Since information transmissions of all K users take place after the joint RS within the same coherence time T_c, the user order for information transmission does not matter. This multi-user RS scheme jointly selects a set of relays for all K users in T_c, and thus each user has an opportunity to communicate with its destination in every T_c. However, if we implement a single-user RS scheme in a multi-user network with round robin scheduling, we need at least KT_c time period to complete one transmission for each user. Therefore, our joint RS scheme is extremely important for user-fairness and ultra-reliable low-latency applications in future wireless networks.

Example 1: Let random channel matrices of a three-user four-relay network be

$$\mathbf{H_1} = \begin{bmatrix} 0.74 & 0.06 & 1.12 & 0.89 \\ 3.08 & 1.65 & 2.64 & 1.14 \\ 1.78 & 0.08 & 1.04 & 3.06 \end{bmatrix};\quad \mathbf{D} = \begin{bmatrix} 0.12 \\ 0.29 \\ 2.28 \end{bmatrix};$$

$$\mathbf{H_2} = \begin{bmatrix} 0.47 & 2.82 & 0.57 & 0.29 \\ 1.97 & 1.93 & 5.71 & 0.54 \\ 3.52 & 1.83 & 2.00 & 1.40 \end{bmatrix};\ \mathbf{I} = \begin{bmatrix} 4.55 \\ 2.05 \\ 0.82 \\ 0.98 \end{bmatrix}.$$

For normalized power and path-loss; and variances $\sigma_r^2 = \sigma_d^2 = 0.1$, $\sigma_i^2 = 1.5$ and $\sigma_h^2 = 1.2$; the corresponding SINR matrix $\mathbf{\Gamma}$, the ORS matrix $\mathbf{\Gamma}_o$ and the SRS matrix $\mathbf{\Gamma}_s$ can be calculated as

$$\mathbf{\Gamma} = \mathbf{\Gamma}_o = \begin{bmatrix} 0.16 & 0.03 & 1.21 & \mathbf{0.82} \\ 0.66 & \mathbf{0.77} & 2.86 & 1.06 \\ 0.38 & 0.04 & \mathbf{0.84} & 0.59 \end{bmatrix};$$

$$\mathbf{\Gamma}_s = \begin{bmatrix} 0.36 & 0.04 & \overset{(1.21)}{\mathbf{0.44}} & 0.22 \\ \overset{(0.66)}{\mathbf{1.52}} & 1.03 & 1.65 & 0.41 \\ 1.11 & 0.05 & 0.65 & \overset{(0.59)}{\mathbf{1.08}} \end{bmatrix}.$$

i) For the ORS, we first sort all entries in $\mathbf{\Gamma}_o$ in descending order and fill a temporary matrix $\mathbf{\Gamma}_o^{(1)}$ starting from the largest until each row and at least $K=3$ columns have entries. The last entry is assigned for the corresponding user (user 2 for R_2), and remove the row and the column. This is repeated until the other two users have a relay assigned by generating $\mathbf{\Gamma}_o^{(2)}$ and $\mathbf{\Gamma}_o^{(3)}$.

$$\mathbf{\Gamma}_o^{(1)} = \begin{bmatrix} - & - & 1.21 & 0.82 \\ - & \mathbf{0.77} & 2.86 & 1.06 \\ - & - & 0.84 & - \end{bmatrix}$$

$$\mathbf{\Gamma}_o^{(2)} = \begin{bmatrix} - & \times & 1.21 & \mathbf{0.82} \\ \times & \times & \times & \times \\ - & \times & 0.84 & - \end{bmatrix}$$

$$\mathbf{\Gamma}_o^{(3)} = \begin{bmatrix} \times & \times & \times & \times \\ \times & \times & \times & \times \\ - & \times & \mathbf{0.84} & \times \end{bmatrix}.$$

This results in $S_1-R_4-D_1$, $S_2-R_2-D_2$ and $S_3-R_3-D_3$ with effective SINRs 0.82, 0.77 and 0.84, respectively, where the minimum SINR is 0.77.

ii) We repeat for the SRS with $\mathbf{\Gamma}_s$, which results in $S_1-R_3-D_1$, $S_2-R_1-D_2$ and $S_3-R_4-D_3$ with effective SINRs 1.21, 0.66 and 0.59, respectively. Thus, the minimum SINR is 0.59. The corresponding SINR of SRS are given on top of the bolded elements.

iii) For the naive scheme, we first select the largest entry of the first row which is assigned for the corresponding user, i.e., user 1 for R_3, and remove the row and the column. This is repeated for the other two users. The selection is $S_1-R_3-D_1$, $S_2-R_4-D_2$ and $S_3-R_1-D_3$ with effective SINRs 1.21, 1.06 and 0.38, respectively, where the minimum SINR is 0.38;

iv) The random RS (no unique selection) may give $S_1-R_1-D_1$, $S_2-R_2-D_2$ and $S_3-R_3-D_3$ with effective SINRs 0.16, 0.77 and 0.84, respectively, where the minimum SINR is 0.16.

This specific example shows the benefit of ORS and SRS in term of user fairness.

III. Performance of Max-Min Fairness SRS Scheme

A. Outage Probability

The SRS matrix $\mathbf{\Gamma_s}$ is generated as in (6). We now sort $\gamma_{s,kn}$'s which are elements of $\mathbf{\Gamma_s}$ in descending order, and map with their corresponding SINRs rates of $\mathbf{\Gamma}$ in (4) as follows:

$$\begin{array}{l} \gamma_s^{(1)} \geq \cdots \geq \gamma_s^{(j)} \geq \cdots \geq \gamma_s^{((K-1)N+1)} \geq \cdots \geq \gamma_s^{(KN)} \\ \downarrow \qquad\quad \downarrow \qquad\quad \downarrow \qquad\quad \downarrow \\ \gamma^{(1)} \quad \cdots \quad \gamma^{(j)} \quad \cdots \quad \gamma^{((K-1)N+1)} \quad \cdots \quad \gamma^{(KN)} \end{array} \tag{7}$$

where $\gamma_s^{(j)}$ is the jth largest entry of $\mathbf{\Gamma_s}$, and $\gamma^{(j)}$ is the corresponding SINR entry in $\mathbf{\Gamma}$ which is not necessarily the jth largest element of $\mathbf{\Gamma}$. According to the RS algorithm, any selected entry of the RS matrix, i.e., in our SRS scheme $\gamma_s^{(j)}$ of $\mathbf{\Gamma_s}$, satisfies the property $1 \leq j \leq (K-1)N+1$. Because, in worse case, the minimum SINR among users is $\gamma^{((N-1)K+1)}$ which occurs when all $\gamma^{((N-1)K+1)} \geq \cdots \geq \gamma^{(NK)}$ are in a same row if $K > N$; or are either in same row or column if $K = N$. Thus, the user k SINR, γ_k, can be $\gamma_k \in \{\gamma^{(1)}, \ldots, \gamma^{((K-1)N+1)}\}$.

Let N_k be the random index of the relay selected for the user k. Then, the outage probability of user k can be given as $P_k = \Pr[\gamma_k \leq \gamma_{th}]$ where γ_{th} is the SINR threshold. Thus, we have

$$\begin{aligned} P_k(\gamma_{th}) &\overset{(a)}{=} \sum_{j=1}^{(K-1)N+1} \Pr[\gamma^{(N_k)} \leq \gamma_{th}, N_k = j] \\ &\overset{(b)}{=} \sum_{j=1}^{(K-1)N+1} \underbrace{\Pr[N_k = j]}_{\triangleq \mathrm{P}_{(j)}} \Pr[\gamma^{(N_k)} \leq \gamma_{th} | N_k = j] \\ &\overset{(c)}{=} \sum_{j=1}^{(K-1)N+1} \mathrm{P}_{(j)} \underbrace{\Pr[\gamma^{(j)} \leq \gamma_{th}]}_{\triangleq F_{\gamma_{\mathrm{m}}^{(j)}}(\gamma_{th})} \\ &\overset{(d)}{=} \sum_{j=1}^{(K-1)N+1} \mathrm{P}_{(j)} F_{\gamma_{\mathrm{m}}^{(j)}}(\gamma_{th}) \end{aligned} \tag{8}$$

where (a) follows as $\gamma_k \in \{\gamma^{(1)}, \ldots, \gamma^{((K-1)N+1)}\}$; (b) follows from the definition of conditional probability; (c) is because N_k is independent of the values $(\gamma^{(j)})_{j=1}^{NK}$ (N_k only depends on their positions within the matrix $\mathbf{\Gamma_s}$); and (d) follows as each $\gamma^{(j)}$ corresponds to a user pair and a selected relay, and thus, without loss of generality, we write $\gamma_{\mathrm{m}}^{(j)}$ to denote the value $\min(\gamma_{kn,1}^{(j)}, \gamma_{nk,2}^{(j)})$ corresponding to $\gamma^{(j)}$ as per (3).

Theorem 1: For a FD network with K users and N relays, the outage probability of each user with SRS scheme given in (6) can be given as

$$P_o = 1 - \sum_{j=1}^{(K-1)N+1} \sum_{q=0}^{KN-j} \frac{(KN)! \mathrm{P}_{(j)} (-1)^q \binom{KN-j}{q}}{\kappa\, \sigma_f^2 \mu\, \sigma_g^2 (j-1)! (KN-j)!} \mathcal{J}\left(\kappa, \mu, a, b, \sigma_f, \sigma_g, \lambda_u, \lambda_v, \gamma_{th}\right) \tag{9}$$

where the function $\mathcal{J}\left(\kappa, \mu, a, b, \sigma_f, \sigma_g, \lambda_u, \lambda_v, z\right)$, denoted as $\mathcal{J}$ for the sake of brevity, which depends the RSI model and the availability of the direct link can be given for four cases as follows. Proof is in Appendix A.

Case I: RSI Model I with Direct Link

$$\mathcal{J} = \begin{cases} \hat{\mathcal{I}}_1\left(\frac{\kappa z}{a}, \frac{\mu z}{b}, \lambda_c(j+q), \lambda_u, \lambda_v, \frac{1}{\mu\sigma_g^2}\right) \\ +\hat{\mathcal{I}}_2\left(\frac{\mu z}{b}, \frac{\kappa z}{a}, \lambda_c(j+q), \lambda_v, \lambda_u, \frac{1}{\kappa\sigma_f^2}\right), \frac{\kappa}{a} \geq \frac{\mu}{b} \\ \hat{\mathcal{I}}_2\left(\frac{\kappa z}{a}, \frac{\mu z}{b}, \lambda_c(j+q), \lambda_u, \lambda_v, \frac{1}{\mu\sigma_g^2}\right) \\ +\hat{\mathcal{I}}_1\left(\frac{\mu z}{b}, \frac{\kappa z}{a}, \lambda_c(j+q), \lambda_v, \lambda_u, \frac{1}{\kappa\sigma_f^2}\right), \frac{\kappa}{a} < \frac{\mu}{b} \end{cases} \tag{10}$$

where $\lambda_c = \left(\frac{1}{\kappa\sigma_f^2} + \frac{1}{\mu\sigma_g^2}\right)$; $\hat{\mathcal{I}}_1(\theta, \phi, \nu, \tau, \varphi, \rho)$ and $\hat{\mathcal{I}}_2(\theta, \phi, \nu, \tau, \varphi, \rho)$ are

$$\begin{aligned} \hat{\mathcal{I}}_1 &= \left(\frac{\tau e^{-\theta\nu}}{\nu\rho(\theta\nu+\tau)} - \frac{\tau(\phi\nu+\varphi)^{-1} e^{-\theta\nu}\phi^3\, e^{-\frac{\varphi(\theta-\phi)}{\phi}}}{(\phi\rho+\varphi)(\theta(\phi\nu+\varphi)+\phi\tau)}\right) \\ \hat{\mathcal{I}}_2 &= \frac{\varphi\left(\frac{\theta e^{\tau - \frac{\phi(\theta\nu+\tau)}{\theta}}}{\theta(\nu-\rho)+\tau} + \frac{\tau e^{-\theta\nu+\theta\rho-\phi\rho}}{(\nu-\rho)(\theta(\nu-\rho)+\tau)} - \frac{e^{-\phi\nu}}{\nu-\rho}\right)}{\rho(\phi\rho+\varphi)} \\ &\quad + e^{-\phi\nu}\left(\frac{1}{\nu\rho} - \frac{\phi^2}{(\phi\nu+\varphi)(\phi\rho+\varphi)}\right) \\ &\quad - e^{-\phi\nu}\left(\frac{\theta\varphi e^{-\frac{\tau(\phi-\theta)}{\theta}}(\theta(\phi(\nu+\rho)+\varphi)+\phi\tau)}{\rho(\theta\nu+\tau)(\phi\rho+\varphi)(\theta(\phi\nu+\varphi)+\phi\tau)}\right). \end{aligned}$$

Case II: RSI Model II with Direct Link

$$\mathcal{J} = \mathcal{I}\left(\frac{\mu\, z}{b}, z, \lambda_c(j+q), \lambda_v, \frac{1}{\mu\sigma_g^2}, \frac{1}{\kappa\sigma_f^2}\right) \tag{11}$$

where $\mathcal{I}\left(\theta, z, \nu, \tau, \rho, \sigma\right)$ is

$$\mathcal{I} = \frac{e^{-\nu z}}{\nu}\left(\frac{1}{\sigma-\nu} + \frac{1}{\rho}\right) + \frac{\tau e^{-\theta\nu+\theta\sigma-\sigma z}}{\sigma(\nu-\sigma)(\theta(\nu-\sigma)+\tau)}$$

$$+\frac{\theta e^{\tau-z\left(\frac{\tau}{\theta}+\nu\right)}}{\sigma(\theta\nu-\theta\sigma+\tau)}-\frac{\theta^2\ e^{\tau-z\left(\frac{\tau}{\theta}+\nu\right)}}{(\theta\nu+\tau)(\theta\rho+\tau)}-\frac{\theta e^{\tau-\frac{\tau z}{\theta}+\nu(-z)}}{\sigma(\theta\nu+\tau)}$$

Case III: RSI Model I without Direct Link

$$\mathcal{J}=\kappa\sigma_f^2\,\mu\sigma_g^2\,\mathcal{I}\left(\frac{\kappa\,z}{a},z,\lambda_c(j+q),\lambda_u,\frac{1}{\kappa\sigma_f^2},\frac{1}{\mu\sigma_g^2}\right) \quad (12)$$

where $\mathcal{I}(\theta,z,\nu,\tau,\varphi,\rho)$ is

$$\mathcal{I}=\frac{\theta^3\rho(\rho+\varphi-\nu)e^{\tau-\frac{z(\theta\nu+\tau)}{\theta}}}{(\theta\nu+\tau)(\theta\varphi+\tau)(\theta(\nu-\rho)+\tau)}+\frac{\tau e^{-\theta\nu+\theta\rho-\rho z}}{(\nu-\rho)(\theta(\nu-\rho)+\tau)}+\frac{\rho e^{-\nu z}\left(\frac{1}{\rho-\nu}+\frac{1}{\varphi}\right)}{\nu}$$

Case IV: RSI Model II without Direct Link

$$\mathcal{J}=\frac{\kappa\sigma_f^2\,\mu\sigma_g^2}{(j+q)}e^{-(j+q)\left(\frac{1}{\kappa\sigma_f^2}+\frac{1}{\mu\sigma_g^2}\right)z}. \quad (13)$$

B. Asymptotic Analysis for High Transmit Power

Since the interference levels due to the RSI and/or direct links may also be functions of transmit power p, it is important to analyze the impact of interference at high transmit power region ($p\to\infty$). When transmit power increases, outage probability decreases in non-interference scenarios. However, this trend may not hold with interference. According to the system model, we can investigate two cases for the variance of RSI as $\sigma_i^2=\omega p^\nu$ when $\nu=0$ and $\nu=1$. We assume normalized distances ($l_{sr}=l_{rd}=1$) and channel variances ($\sigma_f^2=\sigma_g^2=\sigma_h^2=1$); and the same noise variances at the relay and destination ($\sigma_r^2=\sigma_d^2=\sigma^2$), which are common assumptions for asymptotic analysis. In addition, we define that $r=l_{sr}/l_{sd}$ and find

$$a=b=\frac{p}{\sigma^2};\quad c=\frac{1}{\sigma^2};\ d=r\frac{p}{\sigma^2};$$
$$\kappa=\frac{p/\sigma^2}{1+\sigma_i^2/\sigma^2};\quad\text{and }\mu=\frac{p/\sigma^2}{1+r\,p/\sigma^2}. \quad (14)$$

The asymptotic analysis helps to find the diversity order, d, the decreasing rate of outage probability with the increase in the transmit power p as $p\to\infty$. It is conventionally defined as $d=-\lim_{p\to\infty}\frac{\log P_o}{\log p}$. Further, the array gain can be calculated as $\Omega=\lim_{p\to\infty}\left(P^dP_o\right)^{-1}$. If the diversity order is zero, i.e., $d=0$, we have an outage floor.

Theorem 2: For a FD relay network with K users and N relays:

1) Each user has the diversity order of N when there is no direct links and the variance of RSI is independent of transmit power. The outage probability of each user in (6) can thus be approximated at high transmit power region as
$$P_o=\frac{1}{\Omega p^N}+o\left(\frac{1}{p^{N+1}}\right) \quad (15)$$
where $1/\Omega$ is given at the top of next page.
2) Each user has an outage floor at high transmit power region when there is direct links and/or the variance of RSI is dependent on transmit power. The outage probability of each user in (6) can thus be approximated at high transmit power region as
$$P_o=1-\sum_{j=1}^{(K-1)N+1}\sum_{q=0}^{KN-j}\frac{(KN)!\mathrm{P}_{(j)}(-1)^q}{(j-1)!(KN-j)!}\binom{KN-j}{q}\mathcal{K}(\omega,r,\gamma_{th})+o\left(\frac{1}{p}\right) \quad (16)$$
where $\mathcal{K}(\omega,r,\gamma_{th})$ is given at the top of next page.

For Case I, we only consider scenario $\frac{\kappa}{a}\geq\frac{\mu}{b}$, as scenario $\frac{\kappa}{a}<\frac{\mu}{b}$ happens very rarely.

Proof: See Appendix B. ■

C. Average Throughput

The average throughput, an important wireless network performance measure, is expressed as $\tau=\log_2(1+\mathrm{SINR})$ bits per channel-use [bpcu]. Throughput analysis is particularly important when we consider the same wireless network (Fig. 1) for different transmission protocols which have distinct channel-use utilizations, e.g., HD vs FD radios and orthogonal vs non-orthogonal transmissions. Since the active nodes in each hop are assigned orthogonal channels in each coherence time, the instantaneous throughput of user k becomes $\tau_k=\frac{1}{K}\log_2(1+\gamma_k)$ [bpcu], where γ_k is the user k SINR following the RS. The average throughput can then be written as

$$\bar{\tau}_k=\frac{\int_0^\infty\log_2(1+x)\,f_{\gamma_k}(x)\,dx}{K}=\frac{\int_0^\infty\frac{\bar{F}_{\gamma_k}(x)}{1+x}\,dx}{K\ln(2)} \quad (17)$$

where $f_{\gamma_k}(x)$ is the p.d.f. of γ_k. By employing integration by parts, $\bar{\tau}_k$ can be derived in terms of $\bar{F}_{\gamma_k}(x)$ – the complementary cumulative distribution function (c.c.d.f.) of γ_k. Here the c.c.d.f. may be written as $\bar{F}_{\gamma_k}(x)=1-P_o(\gamma_{th})|_{\gamma_{th}=x}$. Due to the space limitation, we provide analytical expressions only for the RSI Model II, i.e., Case II and Case IV only. The RSI Model I, i.e., Case I and Case III can also be analyzed similarly.

For Case IV - RSI Model II without Direct Link: we have

$$\bar{\tau}_k=\frac{(KN)!}{K\ln(2)}\sum_{j=1}^{(K-1)N+1}\sum_{q=0}^{KN-j}\frac{\mathrm{P}_{(j)}(-1)^q\binom{KN-j}{q}}{e^{-(j+q)\left(\frac{1}{\kappa\sigma_f^2}+\frac{1}{\mu\sigma_g^2}\right)}}\times\frac{\mathrm{Ei}\left(-(j+q)\left(\frac{1}{\kappa\sigma_f^2}+\frac{1}{\mu\sigma_g^2}\right)\right)}{(j-1)!(KN-j)!(j+q)} \quad (18)$$

where this follows by substituting (9) and (13) into (17) with $\int_0^\infty\frac{e^{-ax}}{x+1}=-e^a\mathrm{Ei}(-a)$ for $a>0$ [40, eq. 3.352.4]. Here, $\mathrm{Ei}(\cdot)$ denotes the Exponential integral.

For Case II - RSI Model II with Direct Link: We have

$$\bar{\tau}_k=\frac{(KN)!}{K\ln(2)(\kappa\sigma_f^2)(\mu\sigma_g^2)}\sum_{j=1}^{(K-1)N+1}\sum_{q=0}^{KN-j}\frac{\mathrm{P}_{(j)}(-1)^q\binom{KN-j}{q}}{(j-1)!(KN-j)!}\times\left[\frac{e^\nu\mathrm{Ei}(-\nu)\left(\frac{1}{\nu-\sigma}-\frac{1}{\rho}\right)}{\nu}+\frac{b\tau\mathcal{F}_1\left(\frac{b\sigma+\mu(\nu-\sigma)}{b},\frac{b\tau}{\mu(\nu-\sigma)}\right)}{\mu\sigma(\nu-\sigma)(\nu-\sigma)}\right.$$

$$\frac{1}{\Omega}=\begin{cases}\dfrac{(KN)!\left(z(2\ s+\omega)\right)^N \mathrm{P}_{((K-1)N+1)}}{N!(N-1)!(N(K-1))!}\displaystyle\sum_{q=0}^{N-1}\binom{N-1}{q}\frac{(N(K-1)+q+1)^{N-1}}{(-1)^{N+q+1}}, & \text{Case IV, } \sigma_i^2=\omega\\ \dfrac{(KN)!\mathrm{P}_{((K-1)N+1)}}{N!(N-1)!(N(K-1))!}\displaystyle\sum_{q=0}^{N-1}\binom{N-1}{q}(-1)^{q+1}\mathcal{M}(s,\omega,\gamma_{th}), & \text{Case III, } \sigma_i^2=\omega;\end{cases}$$

$$\begin{aligned}\mathcal{M}(s,\omega,z)=&\frac{(s+\omega)^2\left(\frac{\partial^N}{\partial y^N}\frac{e^{-\frac{syz((2\ s+\omega)(N(K-1)+q+1)+\omega)}{s+\omega}}}{y\omega z(s(2\ N(K-1)+2\ q+1)+\omega(N(K-1)+q+1))+s+\omega}\big|_{y=0}\right)}{s(s(2\ N(K-1)+2\ q+1)+\omega(N(K-1)+q+1))}\\&+\frac{(N(K-1)+q)\left(\frac{\partial^N}{\partial y^N}e^{yz(2\ s+\omega)(-(N(K-1)+q+1))}\big|_{y=0}\right)}{(N(K-1)+q+1)(s(2\ N(K-1)+2\ q+1)+\omega(N(K-1)+q+1))}\\&-\frac{\left(\frac{\partial^N}{\partial y^N}\frac{y^3(y\omega z(2\ s+\omega)(N(K-1)+q+1)+s+\omega)^{-1}e^{yz(2\ s+\omega)(-(N(K-1)+q+1))}}{(y\omega z+1)(y\omega z(s(2\ N(K-1)+2\ q+1)+\omega(N(K-1)+q+1))+s+\omega)}\big|_{y=0}\right)}{(\omega^3\ z^3(2\ s+\omega)(N(K-1)+q))^{-1}e}\end{aligned}$$

$$\mathcal{K}(\omega,r,z)=\begin{cases}\dfrac{1}{rz(j+q)^2+j+q}, & \text{Case I and } \sigma_i^2=\omega\\ \dfrac{z\left(r^2\ z(j+q)+r(j+q+2\omega z+2)+\omega(\omega z(j+q)+j+q+2)\right)+2}{(j+q)(rz+1)(\omega z+1)(z(j+q)(r+\omega)+1)(z(j+q)(r+\omega)+2)}, & \text{Case I and } \sigma_i^2=\omega p\\ \dfrac{1}{rz(j+q)^2+j+q}, & \text{Case II and } \sigma_i^2=\omega\\ \dfrac{\omega(j+q-1)e^{-z(j+q)(r+\omega)}}{(j+q)((j+q)(r+\omega)-\omega)}+\dfrac{re^{-\omega z}((j+q)(r+\omega)-\omega)^{-1}}{(rz(j+q)+\omega z(j+q-1)+1)}\\ \quad-\dfrac{r\omega z^3(j+q-1)(r+\omega)e^{-z(j+q)(r+\omega)-1}}{(rz+1)(rz(j+q)+\omega z(j+q-1)+1)(z(j+q)(r+\omega)+1)}, & \text{Case II and } \sigma_i^2=\omega p\\ \dfrac{1}{\omega z(j+q)^2+j+q}, & \text{Case III and } \sigma_i^2=\omega p\\ \dfrac{e^{-\omega z(j+q)}}{j+q}, & \text{Case IV and } \sigma_i^2=\omega p\end{cases}$$

$$+e^{\tau-\frac{b\tau}{\mu}}\left[\frac{e^{\nu}\mathrm{Ei}(-\nu)}{\nu\rho}-\frac{\mathcal{F}_2\left(\nu,\frac{b\sigma\tau}{\mu\nu\sigma}\right)}{\nu\sigma}+\frac{\left(\frac{b\tau}{\mu\nu}\right)^2\mathcal{F}_1\left(\nu,\frac{b\tau}{\mu\nu}\right)}{\nu\rho\left(\frac{b\tau}{\mu\nu}-\frac{b\tau}{\mu\rho}\right)}\right.$$
$$\left.-\frac{\left(\frac{b\tau}{\mu\rho}\right)^2\mathcal{F}_1\left(\nu,\frac{b\tau}{\mu\rho}\right)}{\nu\rho\left(\frac{b\tau}{\mu\nu}-\frac{b\tau}{\mu\rho}\right)}+\frac{\mathcal{F}_2\left(\nu,\frac{b\tau}{\mu(\nu-\sigma)}\right)}{\sigma(\nu-\sigma)}-\frac{\mathcal{F}_2\left(\nu,\frac{b\sigma\tau}{\mu\nu\sigma}\right)}{\nu\sigma}\right]\Bigg] \tag{19}$$

where $\nu=(j+q)\left(\frac{1}{\kappa\sigma_f^2}+\frac{1}{\mu\sigma_g^2}\right)$, $\tau=\frac{1}{d\sigma_h^2}$, $\rho=\frac{1}{\mu\sigma_g^2}$, $\sigma=\frac{1}{\kappa\sigma_f^2}$, $\mathcal{F}_1(m,a)\triangleq\int_0^\infty\frac{e^{-mz}}{(z+1)(a+z)}dz=\frac{e^{am}\mathrm{Ei}(-ma)}{a-1}+\frac{e^{m}\mathrm{Ei}(-m)}{1-a}$ and $\mathcal{F}_1(m,a)\triangleq\int_0^\infty\frac{ze^{-mz}}{(z+1)(a+z)}dz=\frac{ae^{am}\mathrm{Ei}(-ma)}{1-a}+\frac{e^{m}\mathrm{Ei}(-m)}{a-1}$. Here, (a) follows by substituting (9) and (11) into (17), and subsequent mathematical manipulations with [40]. Since the intermediate steps involve straightforward algebraic manipulations, we omit them.

IV. Further Discussion

A. Half-Duplex Radio

For HD, there is no self-interference at relays. When there are direct links, the maximal ratio combining (MRC) is used at destinations. The equivalent user SINR matrix in (4) is given as

$$\mathbf{\Gamma}^{HD}=\left(\gamma_{kn}^{hd}\right)\in\mathbb{R}^{K\times N} \tag{20}$$

where $\gamma_{kn}^{hd}=\min(x_{kn},y_{kn})+v_k$ with direct link and $\gamma_{kn}^{hd}=\min(x_{kn},y_{kn})$ without direct link. The ORS and SRS matrices for HD mode can be calculated as $\mathbf{\Gamma}_o^{HD}=\mathbf{\Gamma}^{HD}$ and $\mathbf{\Gamma}_s^{HD}=(\min(x_{kn},y_{kn}))\in\mathbb{R}^{K\times N}$, respectively, as $v_k\forall k$ is i.i.d. For a HD network with K users and N relays, performance metrics of each user with SRS scheme can be given as

i) Outage probability:

$$P_o=\begin{cases}\displaystyle\sum_{j=1}^{(K-1)N+1}\sum_{w=0}^{KN-j}\frac{(KN)!\mathrm{P}_{(j)}(-1)^w\binom{KN-j}{w}}{(j-1)!(KN-j)!}\\ \quad\mathcal{T}(\lambda_x,\lambda_y,\lambda_v,\gamma_{th});\quad\text{with direct link;}\\ \displaystyle\sum_{j=1}^{(K-1)N+1}\sum_{i=0}^{j-1}\frac{(-1)^i(KN)!\mathrm{P}_{(j)}\binom{j-1}{i}}{(j-1)!(KN-j)!}\\ \quad\frac{(1-e^{-\gamma_{th}(\lambda_x+\lambda_y)})^{i-j+KN+1}}{(i-j+KN+1)};\quad\text{no direct link.}\end{cases} \tag{21}$$

where $\mathcal{T}(\lambda_x,\lambda_y,\lambda_v,z)$ is

$$\mathcal{T}=\begin{cases}\dfrac{1-e^{-z(j+w)(\lambda_x+\lambda_y)}}{(j+w)}-(\lambda_x+\lambda_y)e^{-z\lambda_v};\\ \qquad(j+w)=\dfrac{\lambda_v}{\lambda_x+\lambda_y},\\ \dfrac{1-e^{-z(j+w)(\lambda_x+\lambda_y)}}{(j+w)}+\dfrac{e^{-z(j+w)(\lambda_x+\lambda_y)}-e^{-\lambda_v z}}{(j+w)-\frac{\lambda_v}{\lambda_x+\lambda_y}};\\ \qquad(j+w)\neq\dfrac{\lambda_v}{\lambda_x+\lambda_y},\end{cases}$$

ii) Asymptotic result:

$$P_o \overset{\frac{1}{p}\to 0}{\longrightarrow} \begin{cases} \sum_{w=0}^{N-1} \frac{\left((2(N(K-1)+w+1))^N - r^N\right)}{(-1)^{N+1+w}(2(N(K-1)+1)-r+2\ w)} \\ \frac{2\ r\binom{N-1}{w}(KN)!\mathrm{P}_{((K-1)N+1)}{\gamma_{th}}^{N+1}}{(k-1)!(N+1)!(N(K-1))!p^{N+1}}; \\ \sum_{i=0}^{N(K-1)} \sum_{w=1}^{N+i} \frac{(KN)!\mathrm{P}_{((K-1)N+1)}\binom{(K-1)N}{i}\binom{i+N}{w}}{(N-1)!(i+N)(-1)^{i+N+w}} \\ \frac{(2\ w\gamma_{th})^N}{N!(N(K-1))!p^N}; \end{cases} \tag{22}$$

where the first expression for with direct link and the second expression for no direct link.

iii) Average throughput:

$$\bar{\tau}_k = \begin{cases} \frac{(KN)!}{2K\ln(2)} \sum_{j=1}^{N(K-1)+1} \sum_{w=0}^{NK-j} \frac{(-1)^w \mathrm{P}_{(j)}\binom{KN-j}{w}}{(j-1)!(NK-j)!} \\ \left[\frac{\mathrm{Ei}(-(j+w)(\lambda_x+\lambda_y))}{e^{-(j+w)(\lambda_x+\lambda_y)}\left[(j+w)-\frac{\lambda_v}{\lambda_x+\lambda_y}\right]}\right. \\ \left. -\frac{e^{\lambda_v}\mathrm{Ei}(-\lambda_v)}{(j+w)-\frac{\lambda_v}{\lambda_x+\lambda_y}} - \frac{\mathrm{Ei}(-(j+w)(\lambda_x+\lambda_y))}{e^{-(j+w)(\lambda_x+\lambda_y)}(j+w)}\right], \\ \frac{(KN)!}{2K\ln(2)} \sum_{j=1}^{N(K-1)+1} \sum_{i=0}^{j-1} \sum_{w=1}^{i-j+NK+1} \frac{(-1)^{i+w}\binom{j-1}{i}}{(j-1)!} \\ \frac{\mathrm{P}_{(j)}\binom{i-j+NK+1}{w}e^{w(\lambda_x+\lambda_y)}\mathrm{Ei}(-w(\lambda_x+\lambda_y))}{(NK-j)!(i-j+NK+1)}, \end{cases} \tag{23}$$

where the first expression for with direct link and the second expression for no direct link.

Since proofs follow same as in Sections III-A, III-B and III-C, we omit them. It is important to note that the HD mode with direct and without direct links achieves diversity order $N+1$ and N, respectively. Further, the fraction $\frac{1}{2K}$ in $\bar{\tau}_k$ is due to HD mode and orthogonal channel assignment for users, which is $\frac{1}{2}K$ for the FD mode.

B. Non-Orthogonal Transmission

With non-orthogonal FD transmission, we need only one time-slot or frequency band. Although time/frequency resources appear to have been saved, inter-user interference may significantly degrade the user SINR. Further, the SINR matrix for a fully-connected $K \times N$ network is not easy to write in general way because the second-hop user SINR depends on the selected relay set. Since each user is supported by only one relay, we have $\frac{N!}{(N-K)!K!}$ possible relay sets, denoted as $\mathcal{R}_s = \{R_{s,1}, \cdots, R_{s,k}, \cdots, R_{s,K}\}$ where $R_{s,k} \in \{R_1, \cdots, R_N\}$ and $s = \{1, \cdots, \frac{N!}{(N-K)!K!}\}$. Here, $R_{s,k}$ which is the relay in set $\mathcal{R}_s$ helps for user k. Abusing the notation, we use $q_{s,k}$ to denote the parameter q of the connection between user k and $R_{s,k}$ where $q \in \{f, g, \tilde{i}\}$. All possible user SINRs connected via any relay in $\mathcal{R}_s$ can be given in matrix form as

$$\mathbf{\Gamma_s} = (\gamma_{s,k}) \in \mathbb{R}^{K\times K} \quad \text{with } \gamma_{s,k} = \min(\gamma_{s,k,1}, \gamma_{s,k,2}) \tag{24}$$

where $\gamma_{s,k,1}$ and $\gamma_{s,k,2}$ are the first-hop and second-hop SINRs which are given, respectively, as

$$\begin{aligned} \gamma_{s,k,1} &= \frac{p\, d_{sr}^{-\eta}|f_{s,k}|^2}{p\, d_{sr}^{-\eta}\sum_{j=1,\ j\neq k}^{K}|f_{s,j}|^2 + |\tilde{i}_{s,k}|^2 + \sigma_r^2} \\ \gamma_{s,k,2} &= \frac{p\, d_{rd}^{-\eta}|g_{s,k}|^2}{p\, d_{rd}^{-\eta}\sum_{j=1,\ j\neq k}^{K}|g_{s,j}|^2 + \sigma_d^2}. \end{aligned} \tag{25}$$

Then, the instantaneous throughput of user k is $\tau_k = \log_2(1+\gamma_{s,k})$ [bpcu].

As we do not know the RS scheme precisely (which is still an open problem), the performance analysis seems more involved than analysis for orthogonal transmission. We thus derive an approximation which may be an upper bound for the outage and a lower bound for the average throughput. We consider single-user (say the first user pair in Fig. 1) RS with N relays where the received signal at each relay includes interference from other $(K-1)$ users, and the received signal at the destination includes interference from other $(K-1)$ relays. Then, the first and second hops SINR are given, respectively, for Model II without direct links (other cases can be treated in the similar way) as

$$\begin{aligned} \gamma_{1n,1} &= \frac{a|f_{1n}|^2}{a\sum_{j=2}^{K}|f_{jn}|^2 + c_1} = \frac{x_{1n}}{u_n + c_1} \\ \gamma_{1n,2} &= \frac{b|g_{1n}|^2}{b\sum_{j=2,n\notin\{2,K\}}^{K}|g_{1j}|^2 + 1} = \frac{y_{1n}}{v+1} \end{aligned} \tag{26}$$

where $a = \frac{p}{l_{sr}^{\eta}\sigma_r^2}$, $b = \frac{p}{l_{rd}^{\eta}\sigma_d^2}$, and $c_1 = 1 + \frac{\sigma_i^2}{\sigma_r^2}$. It is important to note that $\gamma_{1n,1}$ is same as $\gamma_{s,k,1}$ in (25). Since it is difficult to incorporate the selected relay set and the effect of RS scheme, we approximate $\gamma_{s,k,2}$ in (25) by $\gamma_{1n,2}$. Further, x_{1n} and y_{1n} follow exponential distributions $\mathcal{E}xp\,(1/a)$ and $\mathcal{E}xp\,(1/b)$, respectively. Since u_n and v are sum of $(K-1)$ i.i.d. random variables of $\mathcal{E}xp\,(1/a)$ and $\mathcal{E}xp\,(1/b)$, respectively, they follow Gamma distributions $Gamma\,(K-1, 1/a)$ and $Gamma\,(K-1, 1/b)$, respectively. By using fundamental probability theory, we have $F_{\gamma_{1n,1}}(x) = 1 - \frac{e^{-\frac{c_1}{a}x}}{(1+x)^{K-1}}$ and $F_{\gamma_{1n,2}|v}(x) = 1 - e^{-\frac{v+1}{b}x}$. Based on single-user best RS, the instantaneous SINR of the user is

$$\gamma = \max_{n\in\{1,N\}} \min(\gamma_{1n,1}, \gamma_{1n,2}) = \max_{n\in\{1,N\}} \gamma_{1n} \tag{27}$$

where $\gamma_{1n} = \min(\gamma_{1n,1}, \gamma_{1n,2})$. Then, the exact and asymptotic ($p \to \infty$) outage probabilities can be derived, respectively, as

$$\begin{aligned} P_o &= \sum_{j=0}^{N} \frac{(-1)^j\binom{N}{j}e^{-\Delta j\gamma_{th}}}{\left((\gamma_{th}+1)^j(j\gamma_{th}+1)\right)^{K-1}} \\ P_o^{\infty} &\approx \sum_{j=0}^{N} \frac{(-1)^j\binom{N}{j}e^{-\Delta_\infty j\gamma_{th}}}{\left((x+1)^j(j\gamma_{th}+1)\right)^{K-1}} \end{aligned} \tag{28}$$

where $\Delta = \left(\frac{l_{sr}^{\eta}\sigma_r^2}{p}\left(1+\frac{\sigma_i^2}{\sigma_r^2}\right) + \frac{l_{rd}^{\eta}\sigma_d^2}{p}\right)$; $\Delta_\infty = 0$ for $\sigma_i^2 = \omega$; and $\Delta_\infty = \frac{\omega}{\sigma_r^2}$ for $\sigma_i^2 = \omega p$. Although the orthogonal transmission achieves full-diversity order for $\sigma_i^2 = \omega$, the non-orthogonal transmission always approaches to an error floor which is a drawback.

Since all active nodes in each hop transmit simultaneously in each coherence time, the instantaneous throughput of user k becomes $\tau_k = \log_2(1+\gamma_k)$ [bpcu], where γ_k is the user k SINR. Using (17), the average throughput can be derived as

$$\begin{aligned}\bar{\tau} &= \frac{1}{\ln(2)}\sum_{j=1}^{N}\int_0^\infty \frac{(-1)^{j-1}\binom{N}{j}e^{-j\Delta x}}{(x+1)^{j(K-1)+1}(jx+1)^{K-1}}\,dx \\ &= \frac{1}{\ln(2)}\Bigg[\sum_{j=2}^{N}\frac{(-1)^{j-1}\binom{N}{j}}{j^{K-1}}\Bigg[\frac{e^{\Delta j}\Gamma(0,\Delta j)\binom{1-K}{(K-1)j}}{(1/j-1)^{(j+1)(K-1)}} \\ &\quad + \frac{e^{\Delta}\Gamma(0,\Delta)\binom{(1-K)j-1}{K-2}}{(1-1/j)^{(j+1)(K-1)}} + Ne^{\Delta}E_{2K-1}(\Delta) \\ &\quad + \sum_{r=2}^{j(K-1)+1}\frac{e^{\Delta j}E_r(\Delta j)\binom{1-K}{(K-1)j+1-r}}{(1/j-1)^{(j+1)(K-1)+1-r}} \\ &\quad + \sum_{s=2}^{K-1}\frac{e^{\Delta}(\Delta j)^{s-1}\Gamma(1-s,\Delta)\binom{-((K-1)j+1)}{(K-1)-s}}{(1-1/j)^{j(K-1)+1+(K-1)-s}}\Bigg]\Bigg]\end{aligned} \tag{29}$$

where $E_n(z)$ is the exponential integral function and $\Gamma(a,z)$ is the incomplete Gamma function [40]. Since the intermediate steps involve straightforward algebraic manipulations, we omit them.

C. Imperfect CSI

Among different mathematical models for estimation error, we use the model in [41, Sec. III]. Let us consider the true channel gain as $h \sim \mathcal{CN}(0,\sigma_h^2)$ and its estimate as $\hat{h} \sim \mathcal{CN}(0,\sigma_{\hat{h}}^2)$. For a least mean squares estimator, they are related as $h = \hat{h} + \bar{h}$ where $\bar{h}$ is the zero mean Gaussian estimation error with variance of $\sigma_{\bar{h}}^2 = (1-\rho)\sigma_h^2$ and $\rho = \sigma_{\hat{h}}^2/\sigma_h^2$ which relates to the correlation coefficient [42]. Further, $\hat{h}$ and $\bar{h}$ are independent. The channel absolute value, i.e., $|h|$ or $|\hat{h}|$, is Rayleigh distributed. In this section, we consider imperfect CSI incurred by the imperfect channel estimation of f_{kn} and g_{kn}, $\forall k,n$, which can be written as $f_{kn} = \hat{f}_{kn} + \bar{f}_{kn}$ and $g_{kn} = \hat{g}_{kn} + \bar{g}_{kn}$ where $\hat{f}_{kn} \sim \mathcal{CN}(0,\sigma_{\hat{f}}^2)$, $\hat{g}_{kn} \sim \mathcal{CN}(0,\sigma_{\hat{g}}^2)$, and the Gaussian estimation errors $\bar{f}_{kn}$ and $\bar{g}_{kn}$ have zero means and variances $\sigma_{\bar{f}}^2 = (1-\rho_f)\sigma_f^2$ and $\sigma_{\bar{g}}^2 = (1-\rho_g)\sigma_g^2$, respectively, where correlation coefficients are $\rho_f = \sigma_{\hat{f}}^2/\sigma_f^2$ and $\rho_g = \sigma_{\hat{g}}^2/\sigma_g^2$. Further, the amplitudes $|\hat{f}_{kn}|$ and $|\hat{g}_{kn}|$ are Rayleigh distributed rvs. Following Section II-B, the receive SINRs of the first and second hops can be given, respectively, as

$$\begin{aligned}\hat{\gamma}_{kn,1} &= \begin{cases}\dfrac{\hat{a}\hat{\alpha}_{kn}}{1+\hat{c}\epsilon_n} = \dfrac{\hat{x}_{kn}}{1+\hat{u}_n}; & \text{Model-I;}\\ \dfrac{\hat{a}\hat{\alpha}_{kn}}{1+\hat{c}\sigma_i^2} = \dfrac{\hat{x}_{kn}}{1+\hat{c}\sigma_i^2}; & \text{Model-II,}\end{cases}\\ \hat{\gamma}_{kn,2} &= \begin{cases}\dfrac{\hat{b}\hat{\beta}_{kn}}{1+\hat{d}\delta_k} = \dfrac{\hat{y}_{kn}}{1+\hat{v}_k}; & \text{with direct link;}\\ \hat{b}\hat{\beta}_{kn} = \hat{y}_{kn}; & \text{without direct link,}\end{cases}\end{aligned} \tag{30}$$

where $\hat{a} = \frac{p}{l_{sr}^{\eta}\hat{\sigma}_r^2}$, $\hat{c} = \frac{1}{\hat{\sigma}_r^2}$, $\hat{\sigma}_r^2 = \left(\frac{p}{l_{sr}^{\eta}}\sigma_{\bar{f}}^2 + \sigma_r^2\right)$, $\hat{b} = \frac{p}{l_{rd}^{\eta}\hat{\sigma}_d^2}$, $\hat{d} = \frac{p}{l_{sd}^{\eta}\hat{\sigma}_d^2}$ and $\hat{\sigma}_d^2 = \left(\frac{p}{l_{rd}^{\eta}}\sigma_{\bar{g}}^2 + \sigma_d^2\right)$. We also have rvs: $\hat{\alpha}_{kn} = |\hat{f}_{kn}|^2$, $\hat{\beta}_{kn} = |\hat{g}_{kn}|^2$, $\hat{x}_{kn} = \hat{a}\hat{\alpha}_{kn}$, $\hat{y}_{kn} = \hat{b}\hat{\beta}_{kn}$, $\hat{u}_n = \hat{c}\epsilon_n$ and $\hat{v}_k = \hat{d}\delta_k$, which follow exponential p.d.f. as in (2). The parameter λ for $Z \in \{\hat{x}_{kn}, \hat{y}_{kn}, \hat{u}_n, \hat{v}_k\}$ denoted by $\lambda \in \{\lambda_{\hat{x}}, \lambda_{\hat{y}}, \lambda_{\hat{u}}, \lambda_{\hat{v}}\}$, respectively, may have $\lambda_{\hat{x}} = \frac{1}{\hat{a}\sigma_{\hat{f}}^2}$, $\lambda_{\hat{y}} = \frac{1}{\hat{b}\sigma_{\hat{g}}^2}$, $\lambda_{\hat{u}} = \frac{1}{\hat{c}\sigma_i^2}$, and $\lambda_{\hat{v}} = \frac{1}{\hat{d}\sigma_h^2}$.

The end-to-end SINR of user k helped by R_n is given by $\hat{\gamma}_{kn} = \min(\hat{\gamma}_{kn,1}, \hat{\gamma}_{kn,2})$. Thus, the user SINR matrix connected via any relay under imperfect CSI can be given in matrix form as

$$\hat{\mathbf{\Gamma}} = (\hat{\gamma}_{kn}) \in \mathbb{R}^{K\times N} \quad \text{where } \hat{\gamma}_{kn} = \min(\hat{\gamma}_{kn,1}, \hat{\gamma}_{kn,2}). \tag{31}$$

With imperfect CSI of f_{kn} and g_{kn} and no instantaneous CSI of h_k and $\tilde{i}_n$ but their partial knowledge (σ_h^2 and σ_i^2 and known distances), the SRS matrix $\hat{\mathbf{\Gamma}}_s$ is defined as

$$\hat{\mathbf{\Gamma}}_s \triangleq (\hat{\gamma}_{s,kn}) \in \mathbb{R}^{K\times N}; \quad \hat{\gamma}_{s,kn} = \min\left(\hat{\kappa}\,\hat{\alpha}_{kn}, \hat{\mu}\,\hat{\beta}_{kn}\right); \tag{32}$$

where

$$\hat{\kappa} = \frac{\hat{a}}{1+\hat{c}\sigma_i^2}; \quad \text{and } \hat{\mu} = \begin{cases}\dfrac{\hat{b}}{1+\hat{d}\sigma_h^2}; & \text{direct;}\\ \hat{b}; & \text{no direct.}\end{cases}$$

Remark: If we replace rvs $\{\alpha_{kn}, \beta_{kn}, x_{kn}, y_{kn}, u_n, v_k\}$ in (1) and (6) by $\{\hat{\alpha}_{kn}, \hat{\beta}_{kn}, \hat{x}_{kn}, \hat{y}_{kn}, \hat{u}_n, \hat{v}_k\}$; and set of parameters $\{a,\ c,\ \sigma_r^2,\ b,\ d,\ \sigma_d^2,\ \kappa,\ \mu\}$ in (1) and (6) by $\{\hat{a},\ \hat{c},\ \hat{\sigma}_r^2,\ \hat{b},\ \hat{d},\ \hat{\sigma}_d^2,\ \hat{\kappa},\ \hat{\mu}\}$, respectively, we get (30) and (32). Since corresponding rvs in both sets also follow the similar distributions, the outage probability and average throughput of all cases can be deduced from analytical results in Section III being replaced by respective parameters. Therefore, we omit the derivation and do not present expressions for all cases.

However, to clearly show the effect of imperfect CSI on FD RS, as an example, we consider Case IV (RSI Model II and no direct links). For imperfect CSI, with the aid of (9), (13) and respective parameter substitutions, the outage probability of each user is

$$\hat{P}_o = 1 - \sum_{j=1}^{(K-1)N+1}\sum_{q=0}^{KN-j}\frac{(KN)!\mathrm{P}_{(j)}(-1)^q\binom{KN-j}{q}}{(j+q)(j-1)!(KN-j)!} \times e^{-(j+q)\left(\frac{\frac{p}{l_{sr}^{\eta}}\sigma_{\bar{f}}^2+\sigma_i^2+\sigma_r^2}{\frac{p}{l_{sr}^{\eta}}\sigma_{\hat{f}}^2} + \frac{\frac{p}{l_{rd}^{\eta}}\sigma_{\bar{g}}^2+\sigma_d^2}{\frac{p}{l_{rd}^{\eta}}\sigma_{\hat{g}}^2}\right)\gamma_{th}}. \tag{33}$$

Recall that $\sigma_{\bar{f}}^2 = (1-\rho_f)\sigma_f^2$, $\sigma_{\bar{g}}^2 = (1-\rho_g)\sigma_g^2$, $\rho_f = \sigma_{\hat{f}}^2/\sigma_f^2$ and $\rho_g = \sigma_{\hat{g}}^2/\sigma_g^2$. Then, the outage probability of each user can be approximated at high transmit power region as $p \to \infty$

$$\hat{P}_o^{\infty} = 1 - \sum_{j=1}^{(K-1)N+1}\sum_{q=0}^{KN-j}\frac{(KN)!\mathrm{P}_{(j)}(-1)^q\binom{KN-j}{q}}{(j+q)(j-1)!(KN-j)!} \times e^{-(j+q)\Lambda_{\infty}\gamma_{th}} + o\left(\frac{1}{p}\right) \tag{34}$$

where $\Lambda_{\infty} = \left(\frac{1}{\rho_f} + \frac{1}{\rho_g} - 2\right)$ for $\sigma_i^2 = \omega$ and $\Lambda_{\infty} = \left(\frac{1}{\rho_f} + \frac{1}{\rho_g} - 2 + \frac{\omega l_{sr}^{\eta}}{\sigma_{\hat{f}}^2}\right)$ for $\sigma_i^2 = \omega p$. Each user has an outage

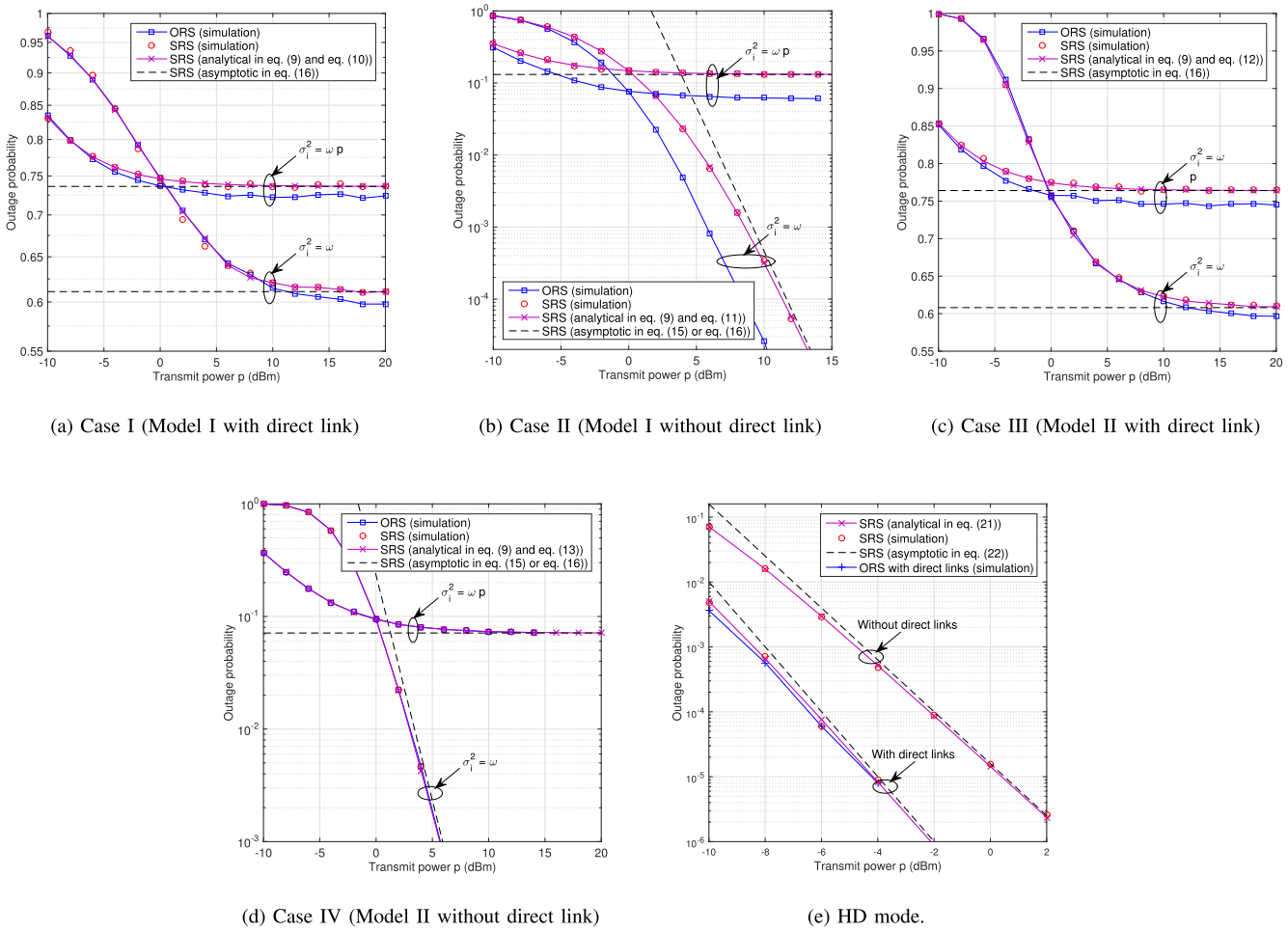

(a) Case I (Model I with direct link)

(b) Case II (Model I without direct link)

(c) Case III (Model II with direct link)

(d) Case IV (Model II without direct link)

(e) HD mode.

Fig. 2. Variation of outage probability with transmit power for FD (Cases I-IV) and HD modes.

floor as the transmit power increases because the variance of channel estimation error enhances with p. Note that we achieve full diversity order with perfect CSI (see (15)) for $\sigma_i^2 = \omega$, as given by

$$\bar{\tau}_k^{\infty} \approx \frac{(KN)!}{K\ln(2)} \sum_{j=1}^{(K-1)N+1} \sum_{q=0}^{KN-j} \frac{\mathrm{P}_{(j)}(-1)^q \binom{KN-j}{q}}{e^{-(j+q)\Lambda_\infty}(j-1)!} \times \frac{\mathrm{Ei}\left(-(j+q)\Lambda_\infty\right)}{(KN-j)!(j+q)}. \quad (35)$$

V. Numerical Results and Discussion

This section presents simulation results to validate our analysis, and discusses the performance of different multiple-user FD networks. We set channel variances as $\sigma_f^2 = \sigma_h^2 = \sigma_g^2 = 1$, noise variances as $\sigma_r^2 = \sigma_d^2 = 0.01$, path-loss exponent $\alpha = 3$ and threshold $\gamma_{th} = 5\,\mathrm{dB}$. To benchmark our proposed SRS scheme, we also simulate the performance of the ideal ORS, where the relay selector has global CSI, i.e., CSI of all f_{kn}, g_{kn}, h_k and $\tilde{i}_n$, $\forall k, n$.

A. Outage Result Verification and Cases I-IV Comparison

Fig. 2 shows outage probabilities of all four cases with transmit power of three-user four-relay network for $\omega = 0.2$ and normalized path-losses. This figure helps verify the analysis. For FD mode, the outage probability of SRS is calculated with (9) using (10)-(13) for Case I to Case IV, respectively; and the asymptotic outage probability of SRS is calculated with (15) or (16). Several observations are gained from Fig. 2: i) For the entire simulated power range, our analytical results closely match with the simulation results for SRS, which confirms Theorem 1 and the accuracy of our analysis; ii) Derived asymptotic results approach simulated results at high p, which confirms the validity of our asymptotic analysis and Theorem 2; iii) While Case II and Case IV with $\sigma_i^2 = \omega$ have diversity order four which is the full-diversity order, other cases exhibit an outage floor because self-interference and/or direct-path interference depend on p; iv) For Cases I, II, and III, the ORS outperforms SRS because instantaneous channel varying effects of direct and/or interference channels are considered in the ORS scheme. Performance gaps between them are given in Table I. While the $\sigma_i^2 = \omega$ case has better performance than the $\sigma_i^2 = \omega\, p$ case, the former exhibits small performance gap as well. Although Case II with $\sigma_i^2 = \omega\, p$ has a higher performance gap than that under Case I or Case III, its overall outage performance is higher than Case I or Case III. It is important to note that both ORS and SRS have similar performance in Case IV because there

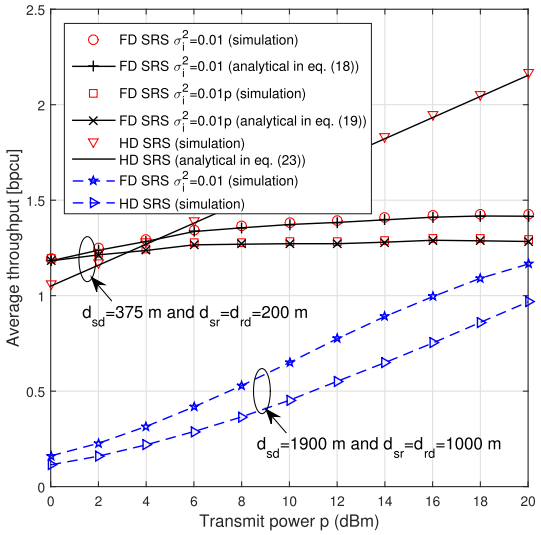

(a) Case III (with direct link).

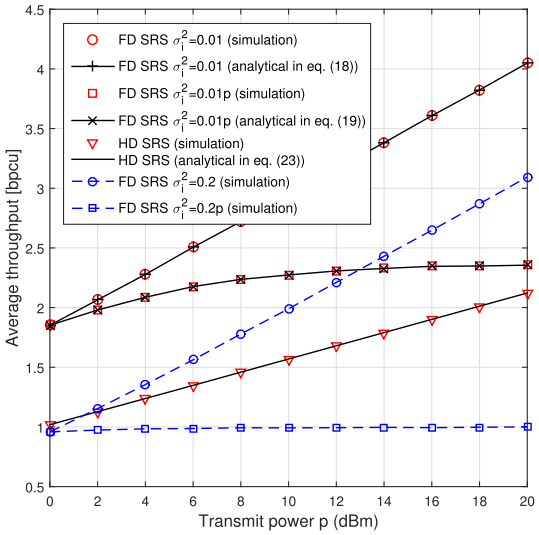

(b) Case IV (without direct link).

Fig. 3. Throughput with transmit power of Model II for FD and HD when $K = 3$ and $N = 4$.

TABLE I

PERFORMANCE GAP BETWEEN THE ORS AND SRS AT $p = 10$ dBm FOR THE FD MODE

	Case I	Case II	Case III	Case IV
$\sigma_i^2 = \omega$	0.0059	0.0003	0.0073	0
$\sigma_i^2 = \omega p$	0.0138	0.0708	0.0189	0

is no direct link and also no channel randomness with self-interference; and v) The network is almost in 75% outage in Case I and Case III with $\sigma_i^2 = \omega p$ for both ORS and SRS as interference power increases with more weight than the signal power when transmit power increases. Fig. 2e depicts outage probability variations with transmit power of the same network for the HD mode. Our exact and asymptotic analytical results match with the simulation for SRS, where diversity orders are four and five without and with direct links, respectively. Although the HD mode outperforms the respective FD modes, e.g., in Figs 2c and 2d for these selected parameters, this may not be a common observation for all scenarios/system parameters.

B. Throughput Result Verification and HD/FD Comparison

Fig. 3 shows the average throughput with transmit power for the FD mode with Model II ($\omega = 0.01$) and HD mode of a three-user four-relay network. To keep the figure less busy, we only consider SRS because SRS and ORS have same or have very close performance. The simulated average throughput is calculated with 10^4 channel realizations. The value of path-loss is 140 dB for the first kilometer of each hop. In Fig. 3a, we consider two direct-link scenarios: i) $l_{sd} = 375$ m, $l_{sr} = l_{rd} = 200$ m; and ii) $l_{sd} = 1.9$ km, $l_{sr} = l_{rd} = 1$ km. For the first scenario, we plot both analytical and simulated results. Our analytical results closely match with the simulations, which confirms the accuracy of our analysis. It is interesting to see that the HD throughput increases with p due to an interference-free transmission. However, the FD mode has a throughput floor due to the introduction of direct-link and/or RSI interference. Therefore, the HD mode outperforms FD mode when $p > 3.3$ dBm for $\sigma_i^2 = 0.01\ p$ and $p > 4.5$ dBm for $\sigma_i^2 = 0.01$ where these crossover p values can be numerically calculated by using eqs. (18), (19) and (23). Further, $\sigma_i^2 = \omega$ case outperforms $\sigma_i^2 = \omega p$ case which is only by 0.1 bpcu at $p = 10$ dBm. This signals us that even RSI has no effect from p, the direct paths interference can still be the dominant factor on the performance. If we increase distances ($l_{sd} = 1.9$ km, $l_{sr} = l_{rd} = 1$ km). the FD mode with $\sigma_i^2 = \omega$ outperforms the HD mode for the entire simulated power range. In Fig. 3b, we again consider two scenarios without direct links: i) $\sigma_i^2 = 0.01$; and ii) $\sigma_i^2 = 0.2$. For both scenarios, we have a good match between the SRS analytical and simulation results. Further, the FD with $\sigma_i^2 = \omega$ outperforms the HD mode where the FD has very significant improvements with p. In simulated region, while the FD with $\sigma_i^2 = \omega p$ outperforms the HD mode only when $\omega = 0.01$, the FD mode has no throughput gain when $\omega = 0.2p$.

C. Impact of Direct-Links Interference

Fig. 4 shows the average throughput of both FD and HD modes with Model II with SRS. Both figures show that the FD with direct-link throughput approaches the FD without direct-link throughput when l_{sd} increases or σ_h^2 decreases as diminishing the direct link interference. As shown in Fig. 4b, while the FD without direct link outperforms HD with/without direct link, the FD with direct link approaches the HD with direct link at $\sigma_h^2 \approx 1$ and $\sigma_h^2 \approx 0.5$ when $\sigma_i^2 = 0.01$ and $\sigma_i^2 = 0.1$, respectively. If we design an FD relay network assuming no direct links, and unexpectedly direct links are presented with $\sigma_h^2 > 0.5$, we do not gain any benefit with FD mode over HD mode when $\sigma_i^2 \geq 0.1$, even with a proper RS scheme.

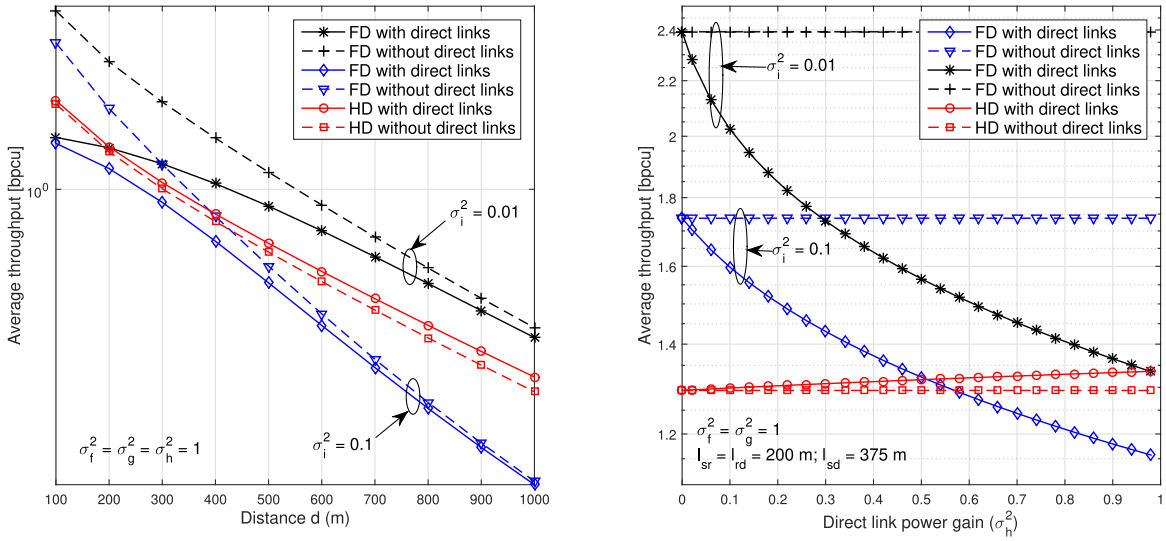

(a) With distance ($l_{sr} = l_{rd} = d$ and $l_{sd} = 1.9d$).

(b) With variance σ_h^2.

Fig. 4. Throughput of Model II for FD and HD modes when $p = 5$ dBm, $K = 3$ and $N = 4$.

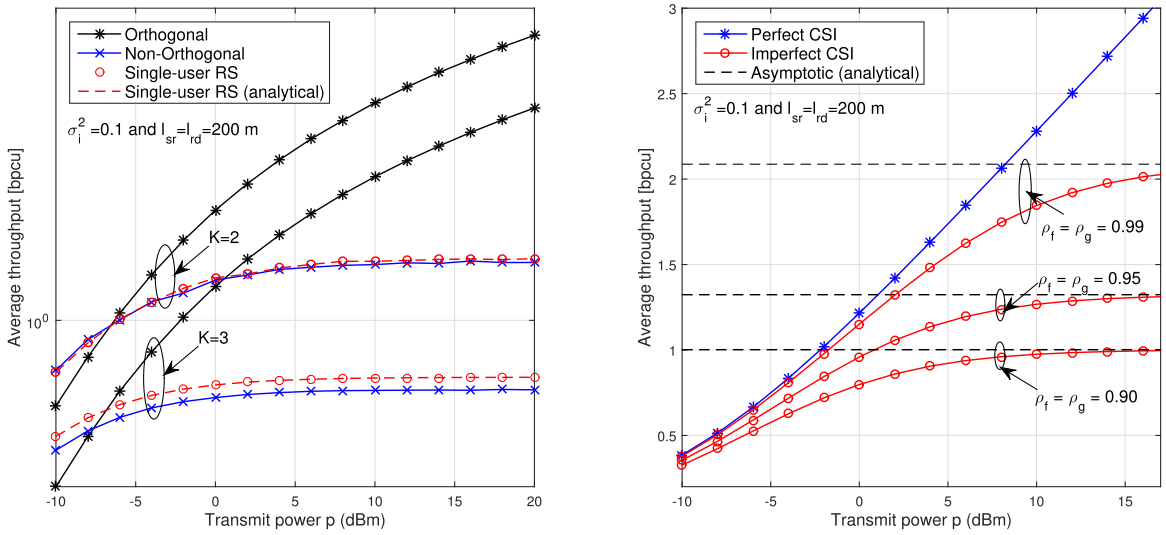

(a) Orthogonal/non-orthogonal transmission.

(b) Perfect/imperfect CSI ($K = 3$).

Fig. 5. Throughput of Model II without direct links for FD mode when $N = 4$.

D. Comparisons Between Perfect/Imperfect CSI and Orthogonal/Non-Orthogonal Transmissions

Fig. 5 shows the average throughput with p of Model II without direct links. Fig. 5a compares the impact of non-orthogonal transmission. Figure shows that the orthogonal system outperforms the non-orthogonal one in almost all $p >$-4 dBm. Moreover, the performance of the latter degrades further with the increasing number of users due to enhancement of inter-user interference. Our throughput approximation in (29) tightly matches with simulated non-orthogonal throughput for $K = 2$ and it is also a good upper bound for $K = 3$. As we can expect, the tightness may loose as K increases. Fig. 5b compares the impact of imperfect CSI. While throughput with perfect CSI increases with p, as we prove in (35), imperfect CSI reaches throughput floors 2.09, 1.32 and 1.00 [bpcu] for correlation coefficients $\rho = 0.99$, 0.95 and 0.90, respectively. Moreover, at $p =$10 dBm, we loose around 0.44 [bpcu] with $\rho = 0.99$ (very small estimation error) which is around 20% throughput lost over perfect CSI. Similarly we loose around 44% and 57% with $\rho = 0.95$ and 0.90, respectively.

VI. Conclusions

We have considered the FD RS problem for a network with multiple-user pairs and multiple DF relays. We have sought an RS scheme (unlike random or naive RS) to ensure user fairness by improving the minimum SINR among all users. To this end, we have proposed a sub-optimal RS scheme when the relay selector knows the instantaneous CSI of the source-to-relay and relay-to-destination channels and only the

channel statistics of the RSI and source-to-destination. Thus, this scheme has reduced channel estimation requirements, which will enhance its potential in the context of practical FD relay networks. This scheme, moreover, does become optimal when the RSI channels are Gaussian noise and there are no direct links. We derived analytical outage expressions to reveal that all users achieve the full diversity order only when the self-interference is independent of transmit power and when there are no direct links. In all other cases, there is an outage floor, and that floor level depends on the interference caused by RSI and/or the direct link. Although we expect FD to exceed the throughput of HD, the former suffers significant throughput degradation when the self-interference increases with the transmit power and the source-destination distance shrinks. We also found that even though orthogonal transmission requires more spectrum, it most probably outperforms non-orthogonal transmission even with few users (e.g., two users), which suffers from additional inter-user interference.

This paper opens the door for several future works: i) Derivatives of the proposed scheme for multiple-user FD networks can be developed for various new 5G configurations and applications, such as NOMA, energy harvesting, cognitive radio, and others; ii) This work shows that the performance of multiple-user networks depends on myriad of parameters. However, there is no clear-cut way to determine when to switch between FD and HD modes or between orthogonal and non-orthogonal transmissions, which is an open problem; iii) It is important to design transmitter and receiver techniques (e.g., STC and buffering) in order to utilize the benefit of direct link signal; and iv) The RS algorithm can further be extended to a general multi-hop FD relaying networks with no restriction on number of relays, i.e., $K \lesseqgtr N$.

APPENDIX A
PROOF OF THEOREM 1

A. Case I

We calculate $F_{\gamma_{\mathrm{m}}^{(j)}}(\gamma_{th})$ in (8) for the RSI Model I with direct link. According to the SINR of user k given in (3) and individual hop SINRs in (1), we can denote $\gamma_{\mathrm{m}}^{(j)} = \min\left(\frac{x^{(j)}}{1+u^{(j)}}, \frac{y^{(j)}}{1+v^{(j)}}\right)$ where $x^{(j)}$, $u^{(j)}$, $y^{(j)}$ and $v^{(j)}$ follow distributions as in (2). Then, we have

$$\begin{aligned} F_{\gamma_{\mathrm{m}}^{(j)}}(z) &= \Pr\left[\min\left(\frac{x^{(j)}}{1+u^{(j)}}, \frac{y^{(j)}}{1+v^{(j)}}\right) \le z\right] \\ &= 1 - \Pr\left[\frac{x^{(j)}}{1+u^{(j)}} > z, \frac{y^{(j)}}{1+v^{(j)}} > z\right] \\ &\overset{(a)}{=} 1 - \mathbb{E}\Bigg[F_{u^{(j)}}\left(\frac{x^{(j)}}{z} - 1\right) F_{v^{(j)}}\left(\frac{y^{(j)}}{z} - 1\right) \\ &\qquad \mathbb{1}\left(x^{(j)} > z\right) \mathbb{1}\left(y^{(j)} > z\right)\Bigg] \\ &\overset{(b)}{=} \mathbb{E}\Bigg[F_{u^{(j)}}\left(\frac{\kappa\,\alpha^{(j)}}{\left(\frac{\kappa}{a}\right) z} - 1\right) F_{v^{(j)}}\left(\frac{\mu\,\beta^{(j)}}{\left(\frac{\mu}{b}\right) z} - 1\right) \\ &\qquad \mathbb{1}\left(\kappa\,\alpha^{(j)} > \frac{\kappa\, z}{a}\right) \mathbb{1}\left(\mu\,\beta^{(j)} > \frac{\mu\, z}{b}\right)\Bigg] \end{aligned} \tag{36}$$

where (a) follows as $u^{(j)}$ and $v^{(j)}$ are independent for given $x^{(j)}$ and $y^{(j)}$; and it also follows as $u^{(j)} > 0$ and $v^{(j)} > 0$, and $F_{u^{(j)}}(\cdot)$ and $F_{v^{(j)}}(\cdot)$ are c.d.f.s of $u^{(j)}$ and $v^{(j)}$, respectively. Further, (b) follows as $x^{(j)} = a\,\alpha^{(j)}$ and $y^{(j)} = b\,\beta^{(j)}$, and with a simple rearrangement to help the application of the RS criterion in (6). For a given $\gamma_s^{(j)}$, based on (6), $\gamma_{s,kn} = \min\left(\kappa\alpha_{kn}, \mu\beta_{kn}\right)$, we have

$$\begin{aligned} &\left(\kappa\alpha^{(j)}, \mu\beta^{(j)}\right) \\ &\quad = \begin{cases} \left(\gamma_s^{(j)}, \mu\beta^{(j)}_{>\gamma_s^{(j)}}\right); & \text{w.p. } p_1 = \dfrac{\mu\sigma_g^2}{\kappa\sigma_f^2 + \mu\sigma_g^2} \\ \left(\kappa\alpha^{(j)}_{>\gamma_s^{(j)}}, \gamma_s^{(j)}\right); & \text{w.p. } p_2 = \dfrac{\kappa\sigma_f^2}{\kappa\sigma_f^2 + \mu\sigma_g^2} \end{cases} \end{aligned} \tag{37}$$

where 'w.p.' denotes *with probability*, $p_2 = 1 - p_1$, and $\mu\beta^{(j)}_{>\gamma_s^{(j)}}$ and $\kappa\alpha^{(j)}_{>\gamma_s^{(j)}}$ mean that $\mu\beta^{(j)} > \gamma_s^{(j)}$ and $\kappa\alpha^{(j)} > \gamma_s^{(j)}$, respectively. Since $\kappa\alpha^{(j)}$ and $\mu\beta^{(j)}$ are independent and their c.d.f.s are $1 - e^{-\frac{1}{\kappa\sigma_f^2}z}$ and $1 - e^{-\frac{1}{\mu\sigma_g^2}z}$, respectively, the c.d.f. of $\gamma_{s,kn}$ is $F_{\gamma_{s,kn}}(z) = 1 - e^{-\lambda_c z}$ where $\lambda_c = \frac{1}{\kappa\sigma_f^2} + \frac{1}{\mu\sigma_g^2}$. Then, the p.d.f. of $\gamma_{s,kn}$ is $f_{\gamma_{s,kn}}(z) = \lambda_c e^{-\lambda_c z}$. Although $\kappa\alpha^{(j)}$ and $\mu\beta^{(j)}$ are independent but not necessary to be identical, we have i.i.d. $\gamma_{s,kn}$, $\forall n, k$. Thus, the p.d.f. of the jth largest element of $\mathbf{\Gamma}_s$, $\gamma_s^{(j)}$, can be given as[3]

$$f_{\gamma_s^{(j)}}(z) = \sum_{q=0}^{KN-j} \frac{\lambda_c (KN)! (-1)^q \binom{KN-j}{q}}{(j-1)!(KN-j)!} e^{-\lambda_c (j+q) z}. \tag{38}$$

Further, the p.d.f.s of $\alpha_s^{(j)} \triangleq \kappa\alpha^{(j)}_{>\gamma_s^{(j)}}$ and $\beta_s^{(j)} \triangleq \mu\beta^{(j)}_{>\gamma_s^{(j)}}$ are, respectively, as

$$f_{\alpha_s^{(j)}}(z) = \frac{e^{-\frac{1}{\kappa\sigma_f^2}(z - \gamma_s^{(j)})}}{\kappa\sigma_f^2}, \quad f_{\beta_s^{(j)}}(z) = \frac{e^{-\frac{1}{\mu\sigma_g^2}(z - \gamma_s^{(j)})}}{\mu\sigma_g^2}. \tag{39}$$

Then, we can rewrite (36) as

$$\begin{aligned} F_{\gamma_{\mathrm{m}}^{(j)}}(z) = 1 - p_1 &\int_{\frac{\kappa z}{a}}^{\infty} \int_{\max\{t, \frac{\mu z}{b}\}}^{\infty} F_{u^{(j)}}\left(\frac{t}{\frac{\kappa z}{a}} - 1\right) \\ &\times F_{v^{(j)}}\left(\frac{w}{\frac{\mu z}{b}} - 1\right) f_{\beta_s^{(j)}}(w) f_{\gamma_s^{(j)}}(t) dw dt \\ - p_2 &\int_{\frac{\mu z}{b}}^{\infty} \int_{\max\{t, \frac{\kappa z}{a}\}}^{\infty} F_{u^{(j)}}\left(\frac{w}{\frac{\kappa z}{a}} - 1\right) \\ &\times F_{v^{(j)}}\left(\frac{t}{\frac{\mu z}{b}} - 1\right) f_{\alpha_s^{(j)}}(w) f_{\gamma_s^{(j)}}(t) dw dt. \end{aligned} \tag{40}$$

With the aid of (37)-(39), we calculate the first and the second integral terms, $\mathcal{I}_1$ and $\mathcal{I}_2$, in (40), respectively, as (41) and (42), given in the top of next page.

To solve two integrals in (41) and (42), we define a function $\mathcal{I}(\theta, \phi, \vartheta, \tau, \varphi, \rho)$ as

$$\begin{aligned} \mathcal{I}(\theta, \phi, \vartheta, \tau, \varphi, \rho) = &\int_{\theta}^{\infty} \int_{\max\{t, \phi\}}^{\infty} \left(1 - e^{-\tau\left(\frac{t}{\theta} - 1\right)}\right) \\ &\left(1 - e^{-\varphi\left(\frac{w}{\phi} - 1\right)}\right) e^{-\rho(w-t)} e^{-\vartheta t} dw dt. \end{aligned} \tag{43}$$

[3]If we assume different power levels for each node and/or distances between nodes, we have non-identical κ, and μ values. Then, the p.d.f. $f_{\gamma_s^{(j)}}(z)$ results from independent but non-identically distributed (i.n.i.d.) rvs which adds significantly to the complexity.

$$\mathcal{I}_1 = \frac{\lambda_c(KN)!}{\mu\sigma_g^2(j-1)!(KN-j)!}\sum_{q=0}^{KN-j}(-1)^q\binom{KN-j}{q} \times \int_{\frac{\kappa z}{a}}^{\infty}\int_{\max\{t,\frac{\mu z}{b}\}}^{\infty}\left(1-e^{-\lambda_u\left(\frac{t}{\frac{\kappa z}{a}}-1\right)}\right)\left(1-e^{-\lambda_v\left(\frac{w}{\frac{\mu z}{b}}-1\right)}\right)e^{-\frac{1}{\mu\sigma_g^2}(w-t)}e^{-\lambda_c(j+q)t}dwdt \quad (41)$$

$$\mathcal{I}_2 = \frac{\lambda_c(KN)!}{\kappa\sigma_f^2(j-1)!(KN-j)!}\sum_{q=0}^{KN-j}(-1)^q\binom{KN-j}{q} \times \int_{\frac{\mu z}{b}}^{\infty}\int_{\max\{t,\frac{\kappa z}{a}\}}^{\infty}\left(1-e^{-\lambda_v\left(\frac{t}{\frac{\mu z}{b}}-1\right)}\right)\left(1-e^{-\lambda_u\left(\frac{w}{\frac{\kappa z}{a}}-1\right)}\right)e^{-\frac{1}{\kappa\sigma_f^2}(w-t)}e^{-\lambda_c(j+q)t}dwdt \quad (42)$$

Since the integration limit of w depends on θ and ϕ, we analyze $\mathcal{I}(\theta,\phi,\vartheta,\tau,\varphi,\rho)$ for $\theta\geq\phi$ and $\theta<\phi$, denoted as $\mathcal{I}_{\theta\geq\phi}$ and $\mathcal{I}_{\theta<\phi}$, respectively. For $\theta\geq\phi$, we have

$$\mathcal{I}_{\theta\geq\phi} = \int_{\theta}^{\infty}\int_{t}^{\infty}f(w,t)dwdt = \frac{\tau e^{-\theta\vartheta}}{\vartheta\rho(\theta\vartheta+\tau)} - \frac{\tau e^{-\theta\vartheta}\phi^3 e^{-\frac{\varphi(\theta-\phi)}{\phi}}}{(\phi\vartheta+\varphi)(\phi\rho+\varphi)(\theta(\phi\vartheta+\varphi)+\phi\tau)} \quad (44)$$

where the second equality comes by using $\int_{\theta}^{\infty}\int_{t}^{\infty}e^{-pt}e^{-qw}dwdt = \frac{e^{-\theta(p+q)}}{q(p+q)}$. For $\theta<\phi$, we have

$$\begin{aligned}\mathcal{I}_{\theta<\phi} &= \int_{\theta}^{\phi}\int_{\phi}^{\infty}f(w,t)\,dwdt + \int_{\phi}^{\infty}\int_{t}^{\infty}f(w,t)\,dwdt \\ &= \frac{\varphi\left(\frac{\theta e^{\tau-\frac{\phi(\theta\vartheta+\tau)}{\theta}}}{\theta(\vartheta-\rho)+\tau} - \frac{e^{-\phi\vartheta}}{\vartheta-\rho} + \frac{\tau e^{-\theta\vartheta+\theta\rho-\phi\rho}}{(\vartheta-\rho)(\theta(\vartheta-\rho)+\tau)}\right)}{\rho(\phi\rho+\varphi)} \\ &\quad + e^{-\phi\vartheta}\left(\frac{1}{\vartheta\rho} - \frac{\phi^2}{(\phi\vartheta+\varphi)(\phi\rho+\varphi)}\right. \\ &\quad \left. - \frac{\theta\varphi e^{-\frac{\tau(\phi-\theta)}{\theta}}(\theta(\phi(\vartheta+\rho)+\varphi)+\phi\tau)}{\rho(\theta\vartheta+\tau)(\phi\rho+\varphi)(\theta(\phi\vartheta+\varphi)+\phi\tau)}\right) \quad (45)\end{aligned}$$

where the second equality comes by using $\int_{\theta}^{\phi}\int_{\phi}^{\infty}e^{-pt}e^{-qw}dwdt = \frac{(e^{\phi p}-e^{\theta p})e^{-\theta p-\phi(p+q)}}{pq}$. By using (44) and (45), we can solve $\mathcal{I}_1$ and $\mathcal{I}_2$ in (40), and thus, $F_{\gamma_{\mathrm{m}}^{(j)}}(z)$ can be derived in closed-form. Because $\sum_{j=1}^{(K-1)N+1}\mathrm{P}_{(j)}=1$, we can derive the user outage as in (9) and (10).

B. Case II

In this case, we have $\gamma_{\mathrm{m}}^{(j)} = \min\left(\frac{x^{(j)}}{1+c\,\sigma_i^2}, \frac{y^{(j)}}{1+v^{(j)}}\right)$. Then, we can write

$$\begin{aligned}F_{\gamma^{(j)}}(z) &= 1 - p_1\int_{z}^{\infty}\int_{t}^{\infty}F_{v^{(j)}}\left(\frac{w}{\frac{\mu z}{b}}-1\right)f_{\beta_s^{(j)}}(w)f_{\gamma_s^{(j)}}(t)dwdt \\ &\quad - p_2\int_{\frac{\mu z}{b}}^{z}\int_{z}^{\infty}F_{v^{(j)}}\left(\frac{t}{\frac{\mu z}{b}}-1\right)f_{\alpha_s^{(j)}}(w)f_{\gamma_s^{(j)}}(t)dwdt \\ &\quad - p_2\int_{z}^{\infty}\int_{t}^{\infty}F_{v^{(j)}}\left(\frac{t}{\frac{\mu z}{b}}-1\right)f_{\alpha_s^{(j)}}(w)f_{\gamma_s^{(j)}}(t)dwdt \quad (46)\end{aligned}$$

where this follows by applying steps in (36) and (40); and as $\frac{\mu}{b}<1$. These three double integrals can be solved in closed-forms as follows:

$$\begin{aligned}&\int_{\theta}^{\infty}\int_{t}^{\infty}\left(1-e^{-\varphi\left(\frac{w}{\phi}-1\right)}\right)e^{-\rho(w-t)}e^{-\nu t}dwdt \\ &= \frac{e^{-\theta\left(\nu+\frac{\varphi}{\phi}\right)}\left(e^{\frac{\theta\varphi}{\phi}}(\nu\phi+\varphi)(\rho\phi+\varphi)-\nu\rho e^{\varphi}\phi^2\right)}{\nu\rho(\nu\phi+\varphi)(\rho\phi+\varphi)} \\ &\int_{\phi}^{\theta}\int_{\theta}^{\infty}\left(1-e^{-\varphi\left(\frac{t}{\phi}-1\right)}\right)e^{-\psi(w-t)}e^{-\nu t}dwdt \\ &\quad + \int_{\theta}^{\infty}\int_{t}^{\infty}f_2(w,t)dwdt = \frac{\phi^2\ e^{\varphi-\frac{\theta(\nu\phi+\varphi)}{\phi}}}{(\nu\phi+\varphi)(\nu\phi+\varphi-\psi\phi)} \\ &\quad + \frac{\varphi e^{-\theta\psi-\nu\phi+\psi\phi}}{\psi(\nu-\psi)(\nu\phi+\varphi-\psi\phi)} - \frac{e^{-\theta\nu}}{\nu^2-\nu\psi}.\end{aligned}$$

We can then derive the user outage as in (9) and (11).

C. Case III

In this case, we have $\gamma_{\mathrm{m}}^{(j)} = \min\left(\frac{x^{(j)}}{1+u^{(j)}}, y^{(j)}\right)$. Then, we can write

$$\begin{aligned}F_{\gamma^{(j)}}(z) &= 1 - p_1\int_{\frac{\kappa z}{a}}^{z}\int_{z}^{\infty}F_{u^{(j)}}\left(\frac{t}{\frac{\kappa z}{a}}-1\right)f_{\beta_s^{(j)}}(w)f_{\gamma_s^{(j)}}(t)dwdt \\ &\quad - p_1\int_{z}^{\infty}\int_{t}^{\infty}F_{u^{(j)}}\left(\frac{t}{\frac{\kappa z}{a}}-1\right)f_{\beta_s^{(j)}}(w)f_{\gamma_s^{(j)}}(t)dwdt \\ &\quad - p_2\int_{z}^{\infty}\int_{t}^{\infty}F_{u^{(j)}}\left(\frac{w}{\frac{\kappa z}{a}}-1\right)f_{\alpha_s^{(j)}}(w)f_{\gamma_s^{(j)}}(t)dwdt \quad (47)\end{aligned}$$

where this follows by applying steps in (36) and (40); and as $\frac{\kappa}{a}<1$. These double integrals can be solved in closed-forms as in Case II and the user outage can be derived as in (9) and (12).

D. Case IV

In this case, we have $\gamma_{\mathrm{m}}^{(j)} = \min\left(\frac{x^{(j)}}{1+c\,\sigma_i^2}, y^{(j)}\right)$. With the aid of (36) and (40), we can write

$$\begin{aligned}F_{\gamma^{(j)}}(z) &= 1 - \int_{z}^{\infty}\int_{t}^{\infty}\left(p_1 f_{\beta_s^{(j)}}(w) + p_2 f_{\alpha_s^{(j)}}(w)\right)f_{\gamma_s^{(j)}}(t)dwdt. \quad (48)\end{aligned}$$

$$P_o = 1 - \underbrace{\sum_{i=0}^{\infty} \sum_{j=1}^{N(K-1)+1} \sum_{q=0}^{KN-j} \frac{(KN)! \mathrm{P}_{(j)} (-1)^{q+i} \binom{KN-j}{q}}{(j-1)!(KN-j)!i!} \frac{z^i (j+q)^{i-1} (2\ s+\omega)^i}{p^i}}_{\triangleq \mathcal{L}(K,N,p,s,\omega,i)}. \tag{49}$$

After solving this double integral, we can derive the user outage as in (9) and (13).

APPENDIX B
PROOF OF THEOREM 2

A. Proof of Theorem 2-1)

Let us consider P_o in (9) for RSI Model II without direct link with $\sigma_i^2 = \omega$. Then, we have P_o as in (49), given in the top this page.

By using the binomial identity for integers $m \geq 0$ and $s \geq 1$: $\sum_{q=0}^{m} \frac{(-1)^q \binom{m}{q}}{(s+q)} = \frac{(s-1)!m!}{(s+m)!}$ and $\sum_{j=1}^{(K-1)N+1} \mathrm{P}_{(j)} = 1$, we have $\mathcal{L}(K, N, p, s, \omega, 0) = 1$. Further, by using the binomial identities for integers $m \geq 0$: $\sum_{q=0}^{m} q^s (-1)^q \binom{m}{q} = 0$ for $s = 0, 1, \ldots, m-1$ and $\sum_{q=0}^{m} q^s (-1)^q \binom{m}{q} = 1$ for $s = m$, we have $\mathcal{L}(K, N, p, s, \omega, t) = 0$ for $t \in \{1, \ldots, N-1\}$. By using the similar binomial identities, for $i = N$, we have

$$\mathcal{L} = \frac{(KN)! \left(\frac{z(2s+\omega)}{p}\right)^N \mathrm{P}_{((K-1)N+1)}}{N!(N-1)!(N(K-1))!} \sum_{q=0}^{N-1} \frac{\binom{N-1}{q}(N(K-1)+q+1)^{N-1}}{(-1)^{N+q+1}} \tag{50}$$

For $i = t$ where $t \in \{N+1, \ldots, \infty\}$, $\mathcal{L}(K, N, p, s, \omega, t)$ may not be zero. Therefore, with the aid of this discussion, we prove (15) for Case IV with $\sigma_i^2 = \omega$. By using above binomial identities and $\sum_{j=1}^{(K-1)N+1} \mathrm{P}_{(j)} = 1$, and with similar mathematical manipulations, we can prove (15) for Case III with $\sigma_i^2 = \omega$.

B. Proof of Theorem 2-2)

Let us consider the following term in (9) which depends on transmit power p

$$\mathcal{J}_p = \frac{1}{\kappa\, \sigma_f^2 \mu\, \sigma_g^2} \mathcal{J}\left(\kappa, \mu, a, b, \sigma_f, \sigma_g, \lambda_u, \lambda_v, z\right). \tag{51}$$

We substitute $\sigma_f^2 = \sigma_g^2 = \sigma_h^2 = 1$; $a = b = \frac{p}{\sigma^2}$; $c = \frac{1}{\sigma^2}$; $d = r\frac{p}{\sigma^2}$; $\kappa = \frac{p/\sigma^2}{1+\sigma_i^2/\sigma^2}$ and $\mu = \frac{p/\sigma^2}{1+r\,p/\sigma^2}$.

1) Case I: In this case, we consider $\frac{\kappa}{a} \geq \frac{\mu}{b}$ scenario in (10) as $\sigma_i^2 < rp$ may be more frequently valid in practice. By substituting corresponding terms in (51) into (10), we may have

$$\mathcal{J}_p = \frac{(\sigma^2+\sigma_i^2)(rp+\sigma^2)}{p^2} \Bigg[\hat{\mathcal{I}}_1 \Bigg(\frac{z}{1+\frac{\sigma_i^2}{\sigma^2}}, \frac{z}{1+\frac{rp}{\sigma^2}}, \frac{(rp+2\sigma^2+\sigma_i^2)}{p(j+q)^{-1}}, \frac{\sigma^2}{\sigma_i^2}, \frac{\sigma^2}{rp}, r+\frac{\sigma^2}{p} \Bigg) + \hat{\mathcal{I}}_2 \Bigg(\frac{z}{1+\frac{rp}{\sigma^2}}, \frac{z}{1+\frac{\sigma_i^2}{\sigma^2}}, \frac{(rp+2\sigma^2+\sigma_i^2)}{p(j+q)^{-1}}, \frac{\sigma^2}{rp}, \frac{\sigma^2}{\sigma_i^2}, \frac{\sigma^2+\sigma_i^2}{p} \Bigg) \Bigg]. \tag{52}$$

For $\sigma_i^2 = \omega$, the first term of (52) is from (10). Then, we can easily show that it approaches zero when $p \to \infty$. Further, the second term of (52) can be approximated for $\frac{1}{p} \to 0$ with the aid of (10) by using following two terms $\mathcal{J}_{p,1}$ and $\mathcal{J}_{p,2}$ which are given, respectively, as

$$\mathcal{J}_{p,1} \to \frac{e^{-\frac{s(dz(j+q)+1)}{s+\omega}}}{dz(j+q)^2+j+q} \Bigg(e^{\frac{s(dz(j+q)+1)}{s+\omega}} - e^{\frac{s}{s+\omega}} (dz(j+q)+1) + dz(j+q) \Bigg) \tag{53}$$

$$\mathcal{J}_{p,2} \to \frac{e^{-\frac{s(dz(j+q)+1)}{s+\omega}} \left(e^{\frac{s}{s+\omega}} (dz(j+q)+1) - dz(j+q) \right)}{dz(j+q)^2+j+q}. \tag{54}$$

We thus derive $\mathcal{J}_p$ in (51) as $\mathcal{J}_p \approx \mathcal{J}_{p,1} + \mathcal{J}_{p,2}$ which results in $\mathcal{J}_p \approx \frac{1}{rz(j+q)^2+j+q} \triangleq \mathcal{K}(\omega, r, z)$ and proves (16) for Case I with $\sigma_i^2 = \omega$. For $\sigma_i^2 = \omega\, p$, by substituting $\sigma_i^2 = \omega\, p$ into (52) and following similar algebraic manipulations as in Case I with $\sigma_i^2 = \omega$, we can prove (16).

2) Cases II-IV: Following similar manipulations as in Appendix B-B.1, we can prove Cases II-IV. By substituting corresponding terms in (51) into (11); (12); and (13), we can prove for Case II with $\sigma_i^2 = \omega$ and $\sigma_i^2 = \omega\, p$; Case III with $\sigma_i^2 = \omega\, p$; and Case IV with $\sigma_i^2 = \omega\, p$, respectively.

REFERENCES

[1] M. Duarte and A. Sabharwal, "Full-duplex wireless communications using off-the-shelf radios: Feasibility and first results," in *Proc. Conf. Rec. 44th Asilomar Conf. Signals, Syst. Comput.*, Pacific Grove, CA, USA, Nov. 2010, pp. 1558–1562.

[2] L. J. Rodríguez, N. H. Tran, and T. Le-Ngoc, "Performance of full-duplex AF relaying in the presence of residual self-interference," *IEEE J. Sel. Areas Commun.*, vol. 32, no. 9, pp. 1752–1764, Sep. 2014.

[3] S. Hong *et al.*, "Applications of self-interference cancellation in 5G and beyond," *IEEE Commun. Mag.*, vol. 52, no. 2, pp. 114–121, Feb. 2014.

[4] Z. Zhang, K. Long, A. V. Vasilakos, and L. Hanzo, "Full-duplex wireless communications: Challenges, solutions, and future research directions," *Proc. IEEE*, vol. 104, no. 7, pp. 1369–1409, Jul. 2016.

[5] G. Amarasuriya, C. Tellambura, and M. Ardakani, "Two-way amplify-and-forward multiple-input multiple-output relay networks with antenna selection," *IEEE J. Sel. Areas Commun.*, vol. 30, no. 8, pp. 1513–1529, Sep. 2012.

[6] S. Atapattu, Y. Jing, H. Jiang, and C. Tellambura, "Relay selection schemes and performance analysis approximations for two-way networks," *IEEE Trans. Commun.*, vol. 61, no. 3, pp. 987–998, Mar. 2013.

[7] S. Silva, G. Amarasuriya, C. Tellambura, and M. Ardakani, "Relay selection strategies for MIMO two-way relay networks with spatial multiplexing," *IEEE Trans. Commun.*, vol. 63, no. 12, pp. 4694–4710, Dec. 2015.

[8] R. Tannious and A. Nosratinia, "Spectrally-efficient relay selection with limited feedback," *IEEE J. Sel. Areas Commun.*, vol. 26, no. 8, pp. 1419–1428, Oct. 2008.

[9] Q. Xue, A. Pantelidou, and B. Aazhang, "Diversity-multiplexing trade-off analysis of MIMO relay networks with full-duplex relays," in *Proc. Asilomar Conf. Signals, Syst. Comput.*, Pacific Grove, CA, USA, Nov. 2013, pp. 1613–1617.

[10] I. Krikidis, H. A. Suraweera, P. J. Smith, and C. Yuen, "Full-duplex relay selection for amplify-and-forward cooperative networks," *IEEE Trans. Wireless Commun.*, vol. 11, no. 12, pp. 4381–4393, Dec. 2012.

[11] Y. Su, L. Jiang, and C. He, "Joint relay selection and power allocation for full-duplex DF co-operative networks with outdated CSI," *IEEE Commun. Lett.*, vol. 20, no. 3, pp. 510–513, Mar. 2016.
[12] K. Yang, H. Cui, L. Song, and Y. Li, "Efficient full-duplex relaying with joint antenna-relay selection and self-interference suppression," *IEEE Trans. Wireless Commun.*, vol. 14, no. 7, pp. 3991–4005, Jul. 2015.
[13] P. C. Sofotasios, M. K. Fikadu, S. Muhaidat, S. Freear, G. K. Karagiannidis, and M. Valkama, "Relay selection based full-duplex cooperative systems under adaptive transmission," *IEEE Wireless Commun. Lett.*, vol. 6, no. 5, pp. 602–605, Oct. 2017.
[14] C. H. M. de Lima, H. Alves, P. H. J. Nardelli, and M. Latva-Aho, "Effects of relay selection strategies on the spectral efficiency of wireless systems with half- and full-duplex nodes," *IEEE Trans. Veh. Technol.*, vol. 66, no. 8, pp. 7578–7583, Aug. 2017.
[15] H. Cui, M. Ma, L. Song, and B. Jiao, "Relay selection for two-way full duplex relay networks with amplify-and-forward protocol," *IEEE Trans. Wireless Commun.*, vol. 13, no. 7, pp. 3768–3777, Jul. 2014.
[16] Y. Tang, H. Gao, X. Su, and T. Lv, "Joint source-relay selection in two-way full-duplex relay network," in *Proc. IEEE Int. Conf. Commun. Workshops (ICC)*, Kuala Lumpur, Malaysia, May 2016, pp. 577–582.
[17] B. Xia, C. Li, and Q. Jiang, "Outage performance analysis of multi-user selection for two-way full-duplex relay systems," *IEEE Commun. Lett.*, vol. 21, no. 4, pp. 933–936, Apr. 2017.
[18] B. Zhong and Z. Zhang, "Opportunistic two-way full-duplex relay selection in underlay cognitive networks," *IEEE Syst. J.*, vol. 12, no. 1, pp. 725–734, Mar. 2018.
[19] B. Ma, H. Shah-Mansouri, and V. W. S. Wong, "A matching approach for power efficient relay selection in full duplex D2D networks," in *Proc. IEEE Int. Conf. Commun. (ICC)*, Kuala Lumpur, Malaysia, May 2016, pp. 1–6.
[20] H. He, P. Ren, Q. Du, and L. Sun, "Full-duplex or half-duplex? Hybrid relay selection for physical layer secrecy," in *Proc. IEEE 83rd Veh. Technol. Conf. (VTC Spring)*, Nanjing, China, May 2016, pp. 1–5.
[21] D. Wang, R. Zhang, X. Cheng, L. Yang, and C. Chen, "Relay selection in full-duplex energy-harvesting two-way relay networks," *IEEE Trans. Green Commun. Netw.*, vol. 1, no. 2, pp. 182–191, Jun. 2017.
[22] K. H. Liu and T. L. Kung, "Performance improvement for RF energy-harvesting relays via relay selection," *IEEE Trans. Veh. Technol.*, vol. 66, no. 9, pp. 8482–8494, Sep. 2017.
[23] X. Yue, Y. Liu, R. Liu, A. Nallanathan, and Z. Ding, "Full/half-duplex relay selection for cooperative NOMA networks," in *Proc. Global Commun. Conf. (GLOBECOM)*, Singapore, Dec. 2017, pp. 1–6.
[24] S. Atapattu, N. Ross, Y. Jing, Y. He, and J. Evans, "Physical-layer security in full-duplex multi-user relay networks," in *Proc. Int. Conf. Commun. (ICC)*, Kansas City, MO, USA, May 2018, pp. 1–6.
[25] C. Li, B. Xia, Q. Jiang, Y. Yao, and G. Yang, "Achievable rate of the multiuser two-way full-duplex relay system," *IEEE Trans. Veh. Technol.*, vol. 67, no. 5, pp. 4650–4654, May 2018.
[26] A. Mukherjee, "Energy efficiency and delay in 5G ultra-reliable low-latency communications system architectures," *IEEE Netw.*, vol. 32, no. 2, pp. 55–61, Mar./Apr. 2018.
[27] M. Chraiti, W. Ajib, and J. F. Frigon, "Distributed Alamouti full-duplex relaying scheme with direct link," in *Proc. IEEE Global Commun. Conf. (GLOBECOM)*, Atlanta, GA, USA, Dec. 2013, pp. 4020–4025.
[28] L. J. Rodríguez, N. Tran, and T. Le-Ngoc, "Performance evaluation of full-duplex af relaying with direct link under residual self-interference," in *Proc. Int. Conf. Commun. (ICC)*, Sydney, NSW, Australia, Jun. 2014, pp. 5712–5716.
[29] D. P. M. Osorio, E. E. B. Olivo, H. Alves, J. C. S. S. Filho, and M. Latva-Aho, "Exploiting the direct link in full-duplex amplify-and-forward relaying networks," *IEEE Signal Process. Lett.*, vol. 22, no. 10, pp. 1766–1770, Oct. 2015.
[30] H. Shen, W. Xu, and C. Zhao, "Transceiver optimization for full-duplex massive MIMO AF relaying with direct link," *IEEE Access*, vol. 4, pp. 8857–8864, 2016.
[31] S. Atapattu, Y. He, P. Dharmawansa, and J. Evans, "Impact of residual self-interference and direct-link interference on full-duplex relays," in *Proc. IEEE Int. Conf. Ind. Inf. Syst. (ICIIS)*, Peradeniya, Sri Lanka, Dec. 2017, pp. 1–6.
[32] S. Atapattu, Y. Jing, H. Jiang, and C. Tellambura, "Relay selection and performance analysis in multiple-user networks," *IEEE J. Sel. Areas Commun.*, vol. 31, no. 8, pp. 1517–1529, Aug. 2013.
[33] R. Senanayake, S. Atapattu, J. S. Evans, and P. J. Smith, "Decentralized relay selection in multi-user multihop decode-and-forward relay networks," *IEEE Trans. Wireless Commun.*, vol. 17, no. 5, pp. 3313–3326, May 2018.
[34] S. Atapattu, P. Dharmawansa, M. D. Renzo, and J. Evans, "Relay selection in full-duplex multiple-user wireless networks," in *Proc. IEEE Global Commun. Conf. (GLOBECOM)*, Singapore, Dec. 2017, pp. 1–6.
[35] A. Zappone, S. Atapattu, M. D. Renzo, J. Evans, and M. Debbah, "Energy-efficient relay assignment and power control in multi-user and multi-relay networks," *IEEE Wireless Commun. Lett.*, to be published.
[36] R. Li, Y. Chen, G. Y. Li, and G. Liu, "Full-duplex cellular networks," *IEEE Commun. Mag.*, vol. 55, no. 4, pp. 184–191, Apr. 2017.
[37] H. Li *et al.*, "Self-interference cancellation enabling high-throughput short-reach wireless full-duplex communication," *IEEE Trans. Wireless Commun.*, vol. 17, no. 10, pp. 6475–6486, Oct. 2018.
[38] S. Khaledian, F. Farzami, B. Smida, and D. Erricolo, "Robust self-interference cancellation for microstrip antennas by means of phase reconfigurable coupler," *IEEE Trans. Antennas Propag.*, vol. 66, no. 10, pp. 5574–5579, Oct. 2018.
[39] S. Sharma, Y. Shi, Y. T. Hou, and S. Kompella, "An optimal algorithm for relay node assignment in cooperative ad hoc networks," *IEEE/ACM Trans. Netw.*, vol. 19, no. 3, pp. 879–892, Jun. 2010.
[40] I. S. Gradshteyn and I. M. Ryzhik, *Table of Integrals, Series and Products*, 7th ed. San Francisco, CA, USA: Academic, 2007.
[41] C. Wang, T. C.-K. Liu, and X. Dong, "Impact of channel estimation error on the performance of amplify-and-forward two-way relaying," *IEEE Trans. Veh. Technol.*, vol. 61, no. 3, pp. 1197–1207, Mar. 2012.
[42] S. M. Kay, *Fundamentals Statistical Signal Processing: Estimation Theory*. Upper Saddle River, NJ, USA: Prentice-Hall, 1993.

Saman Atapattu (M'14) received the B.Sc. degree in electrical and electronics engineering from the University of Peradeniya, Sri Lanka, in 2003, the M.Eng. degree in telecommunications from the Asian Institute of Technology, Thailand, in 2007, and the Ph.D. degree in electrical engineering from the University of Alberta, Canada, in 2013. He is currently a Research Fellow with the Department of Electrical and Electronic Engineering, The University of Melbourne, Australia. His research interests include wireless communications and signal processing.

Prathapasinghe Dharmawansa (S'05–M'09) received the B.Sc. and M.Sc. degrees in electronic and telecommunication engineering from the University of Moratuwa, Moratuwa, Sri Lanka, in 2003 and 2004, respectively, and the Doctor of Engineering (D.Eng.) degree in information and communications technology from the Asian Institute of Technology, Thailand, in 2007. Subsequently, he joined the Department of Electronic and Computer Engineering, Hong Kong University of Science and Technology as a Research Associate. From 2011 to 2012, he was with the Department of Communication and Networking, Aalto School of Electrical Engineering, Aalto University (formerly Helsinki University of Technology), Finland, as a Post-Doctoral Researcher. From 2012 to 2015, he was with the Department of Statistics, Stanford University, CA, USA. He is currently a Senior Lecturer with the Department of Electronic and Telecommunication Engineering, University of Moratuwa. His research interests are in wireless communications, signal processing, and high-dimensional statistics.

Marco Di Renzo (S'05–A'07–M'09–SM'14) was born in L'Aquila, Italy, in 1978. He received the Laurea *(cum laude)* and Ph.D. degrees in electrical engineering from the University of L'Aquila, Italy, in 2003 and 2007, respectively, and the Doctor of Science (HDR) degree from University Paris-Sud, Paris, France, in 2013. Since 2010, he has been a CNRS Associate Professor (Chargé de Recherche Titulaire CNRS) with the Laboratory of Signals and Systems of Paris-Saclay University, CNRS, CentraleSupélec, Univ Paris Sud. He is an Adjunct Professor with the University of Technology Sydney, Australia, a Visiting Professor with the University of L'Aquila, and a Co-Founder of the university spin-off company WEST Aquila s.r.l., Italy. He serves as an Associate Editor-in-Chief for the IEEE COMMUNICATIONS LETTERS, and an Editor for the IEEE TRANSACTIONS ON COMMUNICATIONS, and the IEEE TRANSACTIONS ON WIRELESS COMMUNICATIONS. He is a Distinguished Lecturer of the IEEE Vehicular Technology Society and the IEEE Communications Society. He is the Project Coordinator of the European-funded projects H2020-MSCA ETN-5Gwireless and H2020-MSCA ETN-5Gaura. He was a recipient of several awards, including the 2013 IEEE-COMSOC Best Young Researcher Award for Europe, Middle East and Africa (EMEA Region), the 2013 NoE-NEWCOM# Best Paper Award, the 2014–2015 Royal Academy of Engineering Distinguished Visiting Fellowship, the 2015 IEEE Jack Neubauer Memorial Best System Paper Award, the 2015–2018 CNRS Award for Excellence in Research and in Advising Doctoral Students, the 2016 MSCA Global Fellowship (declined), the 2017 SEE-IEEE Alain Glavieux Award, and seven best paper awards, such as the 2012 and 2014 IEEE CAMAD, the 2013 IEEE VTC, the 2014 IEEE ATC, the 2015 IEEE ComManTel, the 2017 IEEE SigTelCom, and the 2018 INISCOM.

Chintha Tellambura (F'11) received the B.Sc. degree (Hons.) from the University of Moratuwa, Sri Lanka, the M.Sc. degree in electronics from the King's College, University of London, U.K., and the Ph.D. degree in electrical engineering from the University of Victoria, Canada.

He was with Monash University, Australia, from 1997 to 2002. He is currently a Professor with the Department of Electrical and Computer Engineering, University of Alberta. His current research interests include the design, modeling, and analysis of cognitive radio, heterogeneous cellular networks, 5G wireless networks, and machine learning algorithms.

He has authored or co-authored over 500 journal and conference papers with an h-index of 67 (Google Scholar). In 2011, he was elected as an IEEE Fellow for his contributions to physical layer wireless communication theory. In 2017, he was elected as a fellow of the Canadian Academy of Engineering. He has received the Best Paper Award from the Communication Theory Symposium in 2012 IEEE International Conference on Communications (ICC) in Canada and the 2017 ICC in France. He was a recipient of the prestigious McCalla Professorship and the Killam Annual Professorship from the University of Alberta. He served as an Editor for the IEEE TRANSACTIONS ON COMMUNICATIONS from 1999 to 2011 and the IEEE TRANSACTIONS ON WIRELESS COMMUNICATIONS from 2001 to 2007 and the Area Editor for *Wireless Communications Systems and Theory* from 2007 to 2012.

Jamie S. Evans (S'93–M'98–SM'17) was born in Newcastle, Australia, in 1970. He received the B.S. degree in physics and the B.E. degree in computer engineering from the University of Newcastle, in 1992 and 1993, respectively, and the M.S. and the Ph.D. degrees in electrical engineering from The University of Melbourne, Australia, in 1996 and 1998, respectively. From 1998 to 1999, he was a Visiting Researcher with the Department of Electrical Engineering and Computer Science, University of California at Berkeley, Berkeley. He returned to Australia in 1999, he has held academic positions at the University of Sydney, The University of Melbourne, and Monash University. He is currently a Professor and the Deputy Dean in the Melbourne School of Engineering, The University of Melbourne. His research interests are in communications theory, information theory, and statistical signal processing with a focus on wireless communications networks. He received the University Medal upon his graduation from the University of Newcastle. He received the Chancellor's Prize for excellence for his Ph.D. thesis.